COPY 2

Report No. FAA-RD-75-155
NA-75-153

FAA WJH Technical Center
00090601

IGNITION AND PROPAGATION RATES FOR FLAMES IN A FUEL MIST

C. E. Polymeropoulos

NAFEC
LIBRARY
NOV 2 197
RECEIVED

OCTOBER 1975

INTERIM REPORT

Document is available to the public through the
National Technical Information Service,
Springfield, Virginia 22151

Prepared for

U. S. DEPARTMENT OF TRANSPORTATION
FEDERAL AVIATION ADMINISTRATION
Systems Research & Development Service
Washington, D. C. 20590

NOTICE

This document is disseminated under the sponsorship of the Department of Transportation in the interest of information exchange. The United States Government assumes no liability for its contents or use thereof.

METRIC CONVERSION FACTORS

Approximate Conversions to Metric Measures

Symbol	When You Know	Multiply by	To Find	Symbol
		LENGTH		
in	inches	*2.5	centimeters	cm
ft	feet	30	centimeters	cm
yd	yards	0.9	meters	m
mi	miles	1.6	kilometers	km
		AREA		
in^2	square inches	6.5	square centimeters	cm^2
ft^2	square feet	0.09	square meters	m^2
yd^2	square yards	0.8	square meters	m^2
mi^2	square miles	2.6	square kilometers	km^2
	acres	0.4	hectares	ha
		MASS (weight)		
oz	ounces	28	grams	g
lb	pounds	0.45	kilograms	kg
	short tons (2000 lb)	0.9	tonnes	t
		VOLUME		
tsp	teaspoons	5	milliliters	ml
Tbsp	tablespoons	15	milliliters	ml
fl oz	fluid ounces	30	milliliters	ml
c	cups	0.24	liters	l
pt	pints	0.47	liters	l
qt	quarts	0.95	liters	l
gal	gallons	3.8	liters	l
ft^3	cubic feet	0.03	cubic meters	m^3
yd^3	cubic yards	0.76	cubic meters	m^3
		TEMPERATURE (exact)		
°F	Fahrenheit temperature	5/9 (after subtracting 32)	Celsius temperature	°C

*1 in = 2.54 (exactly). For other exact conversions and more detailed tables, see NBS Misc. Publ. 286, Units of Weights and Measures, Price $2.25, SD Catalog No. C13.10:286.

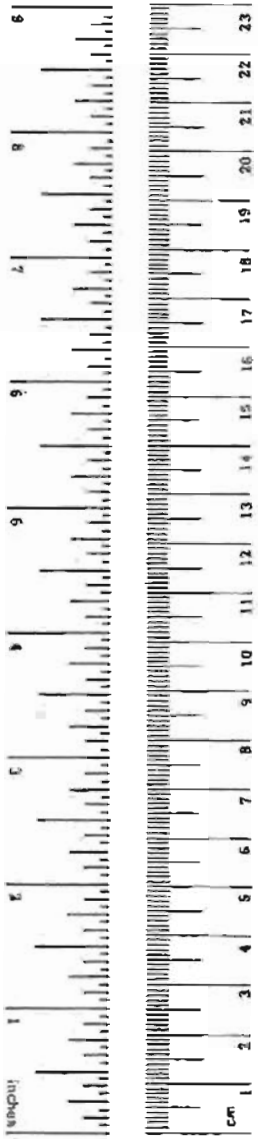

Approximate Conversions from Metric Measures

Symbol	When You Know	Multiply by	To Find	Symbol
		LENGTH		
mm	millimeters	0.04	inches	in
cm	centimeters	0.4	inches	in
m	meters	3.3	feet	ft
m	meters	1.1	yards	yd
km	kilometers	0.6	miles	mi
		AREA		
cm^2	square centimeters	0.16	square inches	in^2
m^2	square meters	1.2	square yards	yd^2
km^2	square kilometers	0.4	square miles	mi^2
ha	hectares (10,000 m^2)	2.5	acres	
		MASS (weight)		
g	grams	0.035	ounces	oz
kg	kilograms	2.2	pounds	lb
t	tonnes (1000 kg)	1.1	short tons	
		VOLUME		
ml	milliliters	0.03	fluid ounces	fl oz
l	liters	2.1	pints	pt
l	liters	1.06	quarts	qt
l	liters	0.26	gallons	gal
m^3	cubic meters	35	cubic feet	ft^3
m^3	cubic meters	1.3	cubic yards	yd^3
		TEMPERATURE (exact)		
°C	Celsius temperature	9/5 (then add 32)	Fahrenheit temperature	°F

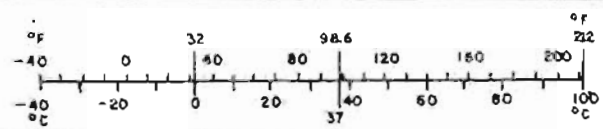

TECHNICAL REPORT STANDARD TITLE PAGE

1. Report No.	2. Government Accession No.	3. Recipient's Catalog No.
FAA-RD-75-155		

4. Title and Subtitle	5. Report Date
IGNITION AND PROPAGATION RATES FOR FLAMES IN A FUEL MIST	April 1975
	6. Performing Organization Code
7. Author(s)	8. Performing Organization Report No.
C. E. Polymeropoulos	FAA-NA-75-153
9. Performing Organization Name and Address Department of Mechanical, Industrial and Aerospace Engineering Rutgers, The State University of New Jersey New Brunswick, New Jersey 08903	10. Work Unit No.
	11. Contract or Grant No. DOT FA 72 NA-746
12. Sponsoring Agency Name and Address U.S. Department of Transportation Federal Aviation Administration Systems Research and Development Service Washington, D.C. 20590	13. Type of Report and Period Covered Interim Report July 1972 - January 1975
	14. Sponsoring Agency Code

15. Supplementary Notes

The contract was administered by the National Aviation Facilities Experimental Center, Atlantic City, New Jersey 08405.

16. Abstract

A mathematical model was developed, which is capable of predicting the burning velocity in polydisperse air-fuel sprays given the initial conditions of the liquid and gas phases. The analytical predictions were tested against previous experimental data, and the agreement was satisfactory.

The burning velocity in polydisperse kerosene-air sprays was measured at constant air-fuel ratio, and for various degrees of atomization of the spray in order to further check the predictions of the mathematical model. The results were also in good agreement with the analytical predictions.

17. Key Words	18. Distribution Statement
Fuels Droplets Sprays Burning Velocity	Document is available to the public through the National Technical Information Service, Springfield, Virginia 22151

19. Security Classif. (of this report)	20. Security Classif. (of this page)	21. No. of Pages	22. Price
Unclassified	Unclassified	61	

Form DOT F 1700.7 (8-69)

PREFACE

This report was prepared by the Mechanical, Industrial and Aerospace Engineering Department at Rutgers, The State University of New Jersey, for the Federal Aviation Administration. From July, 1972, to July, 1973, the work was carried out under the management of Mr. R. A. Russell, and from August, 1973, to January, 1975, under the management of Mr. S. Zinn. The project managers are from the Propulsion-Fire Protection Branch, Aircraft and Airport Safety Division, National Aviation Facilities Experimental Center, Atlantic City, New Jersey.

TABLE OF CONTENTS

	Page
INTRODUCTION	1
Purpose	1
Background	1
MATHEMATICAL MODEL	1
Spray Model	1
General Description and Assumptions	1
Liquid Phase Equations	5
Gas Phase Equations	7
Boundary Conditions	8
Property Calculation	8
Numerical Calculation	9
Results and Discussion	12
Results Obtained Using a Prescribed Gas Temperature as the Ignition Criterion of the Liquid Droplets	12
Choice of the Parameters B_o and E for the Fuel Vapor-Air Mixture	12
Monodisperse Tetralin-Air Sprays	12
Comparison of Calculated Burning Velocities with Available Experimental Data	17
EXPERIMENTAL WORK	17
Previous Work on the Effect of Droplet Size on the Burning Velocity of Liquid-Air Sprays	17
Experimental Apparatus and Procedure	20
Results and Discussion	23
Degree of Atomization in the Sprays Tested	23
Burning Velocity Results	28
CONCLUSIONS	30
APPENDIX A - Procedure for Calculating the Burning Velocity in a Liquid Fuel Spray	31
APPENDIX B - Computer Program Listing	33
REFERENCES	52

LIST OF ILLUSTRATIONS

Figure		Page
1	Schematic Diagram of Fuel Spray and Plane Heat Source	3
2	Burning Velocities of Kerosene Vapor-Air Mixtures	13
3	Burning Velocity vs. Fuel Concentration for Monodisperse Tetralin-Air Sprays. Droplet Diameter is 15μm.	14
4	Drop Diameter vs. Burning Velocity for Monodisperse Tetralin-Air Sprays. Fuel concentration is 69 mg/l.	16
5	Schematic Diagram of the Experimental Apparatus	21
6	Mean Air Velocity and RMS Velocity Fluctuations at the Tube Exit	22
7	Schlieren Images of Flame Front a) Spray A, b) Spray C, c) Spray E	24
8	Schematic Diagram Used for Calculating S_u	25
9	Direct Photographs of Spray Flames a) Spray A, b) Spray C, c) Spray E	26
10	Cumulative Normalized Volume for the Sprays Tested	27

LIST OF TABLES

Table		Page
1	Properties of Kerosene	11
2	Calculated vs. Experimental Burning Velocities	18
3	Droplet Number Densities for Spray A	29
4	Burning Velocities (Air-Fuel/ratio = 18)	29

LIST OF ABBREVIATIONS AND SYMBOLS

B	$B_o T^{\frac{1}{2}}$
B_o	frequency constant
c_p	specific heat of the gas mixture
C_D	drag coefficient
$\bar{d}$	Sauter mean diameter
D	binary diffusion coefficient
E	activation energy
f_i	δf_i before droplet ignition
	α_i, $i = 0, P$, after droplet ignition
h_j	heat transfer coefficient
H	enthalpy
H^o	standard enthalpy of formation
$\dot{H}_s$	spray enthalpy flux
k	thermal conductivity
L	latent heat of vaporization for the fuel
$\dot{m}$	total evaporation rate of the spray
M	molecular weight of the gas mixture
$\dot{M}$	mixture mass flux
n	number of droplet size groups
n_i	mole fraction of species i
N_j	number density of droplet group j
p	pressure
Q	heat of reaction for the fuel
r	radial distance from tube axis
R	tube radius
$\bar{R}$	universal gas constant
R_j	radius of droplet group j
Re_j	Reynolds number of droplet group j
S	defined in equation 29
S_u	experimentally determined burning velocity
T	absolute temperature
T_I	Ignition temperature
T_r	reference temperature
t	time
u'	rms velocity fluctuation
u_j	speed of droplet group j
v	gas speed
V_s	spray volume
w_i	mass rate of production for species i per unit volume
x	downstream distance
Y_i	mass fraction of species i
Z	$z/(\exp(z)-1)$
z	defined in equation 6

Greek Symbols

α_i	stoichiometric mass coefficient for species i
$\Delta\ell$	distance along the flame front
Δr	distance along the tube axis
ε	eddy diffusivity
λ	characteristic turbulent length scale
μ	viscosity of the gas
ν	kinematic viscosity of the gas
ρ	density
ϕ	fuel-air ratio / stoichiometric fuel-air ratio

Subscripts

B	boiling point
F	fuel species
g	gaseous phase
I	ignition condition
i	F, O, P, N refers to the species present
j	droplet size group j
L	downstream boundary
ℓ	liquid
m	denotes grid point
N	neutrals
o	upstream boundary
O	oxidizer
P	products
s	refers to the spray
t	refers to turbulent transport properties

INTRODUCTION

PURPOSE.

The purpose of this research effort was to develop a mathematical model for predicting ignition and propagation rates for flames in a fuel mist.

This report describes the model that was developed, and includes comparisons of the theoretical predictions with experimental data on tetralin-air sprays obtained by previous investigators.

In addition, this report describes experiments that were carried out for measuring burning velocities in kerosene-air sprays, and includes comparisons of experimental data with predicted values from the theoretical model.

BACKGROUND.

The work described in this report is related to the burning of fuel in mist or fine spray form during an aircraft crash, and is aimed at identifying pertinent parameters which control the propagation of a flame in a combustible liquid fuel mist. Since the principal interest is in aircraft crash fire safety, the analysis and experimentation are related to burning under atmospheric conditions and to kerosene based fuels. In addition, experimental data from previous investigators (1-3) who employed tetralin-air sprays are used for comparisons with the theoretical predictions of the present work.

The report consists of two principal parts: the first part describes the mathematical model and the results of the numerical computations that were carried out, while the second part contains a description of experimental work on the effect of droplet size on the burning velocity of polydisperse kerosene-air sprays. Instructions for the use of the computer program for calculating burning velocities, and a listing of the program in the Fortran IV language are found in Appendices A and B, respectively.

The work presented in this report has in part appeared in references (4,5).

MATHEMATICAL MODEL

SPRAY MODEL.

GENERAL DESCRIPTION AND ASSUMPTIONS. Propagation of flame in a dilute liquid fuel spray has been studied by several investigators because of its importance to flame stabilization and spray burning. Burgoyne and Cohen (1) Burgoyne (2), and Mizutani and Ogasawara (3) have measured one-dimensional laminar flame propagation velocities in monodisperse sprays. Their results showed that with very small droplets and very dilute sprays the propagation

mechanism is that of a premixed flame, while with large droplets the mechamism is through a relay transfer of the flame from droplet to droplet. Williams (6), using separate analyses for very small and for large droplets, has obtained satisfactory agreement with the results of Burgoyne et al (1), within the accuracy of the assumptions and the constant property values used in the calculations. Measurements of burning velocities in one-dimensional polydisperse sprays have also been reported (7-10) as well as calculated results for pure vaporization (11), and burning (12) of such sprays. In a recent study Mizutani (13) presented calculations for the burning velocity in turbulent polydisperse sprays neglecting preignition vaporization. There is also a considerable body of work related to liquid fuel rocket combustors which was disucssed by Sutton et al (14). The authors of the last reference also describe their three-dimensional analysis and modeling for the burning of a liquid fuel spray. However, as with most other works related to liquid fuel rockets, their analysis does not address itself directly to the flame propagation problem.

The burning of a liquid fuel spray is a process involving complex transient interactions between the droplets and the surrounding gas phase. The gas flow is usually turbulent, and the spray is distributed among different droplet sizes, which move at different velocities and are randomly distributed in space. To simplify the fluid dynamical calculation, the calculations of spray burning velocities were carried out using a one-dimensional flow model. A dilute spray initially consisting of a stream of air and liquid fuel droplets is assumed to pass through a plane heat source located perpendicular to the flow direction as shown in Figure 1. The heat source both increases the gas temperature to a level that is sufficient to ignite the fuel so that combustion is completed within the domain of the numerical computation, and fixes the position of the flame during the calculations. Under these conditions steady state combustion always takes place downstream from the heat source, provided that the velocity of the gas stream is higher than the burning velocity in the spray. The lowest gas velocity for which the spray can exist in steady state is the burning velocity for normal flame propagation. It also identifies the upstream conditions for "flash-back" from a plane heat source. It should be noted that the results are expected to apply only to cases where the droplet trajectories follow the streamlines of the gas. The mathematical formulation follows the analysis of Williams and Sutton et al (14), and employs the following general assumptions:

1. The gas flow is one-dimensional, steady, at constant pressure, and obeys the ideal gas equation. Thermal radiation effects are neglected.

2. The gaseous mixture in each section is homogeneous. This implies that there is an instantaneous mixing of the species, and that the presence of the liquid phase affects the gas flow only through source and sink terms for species produced or consumed around the droplets.

3. The mixture flow is adiabatic except at the location of the plane heat source.

4. The spray is dilute, and the distribution of droplet sizes is described in terms of a finite number of size groups. There is no interaction between droplets during evaporation or combustion.

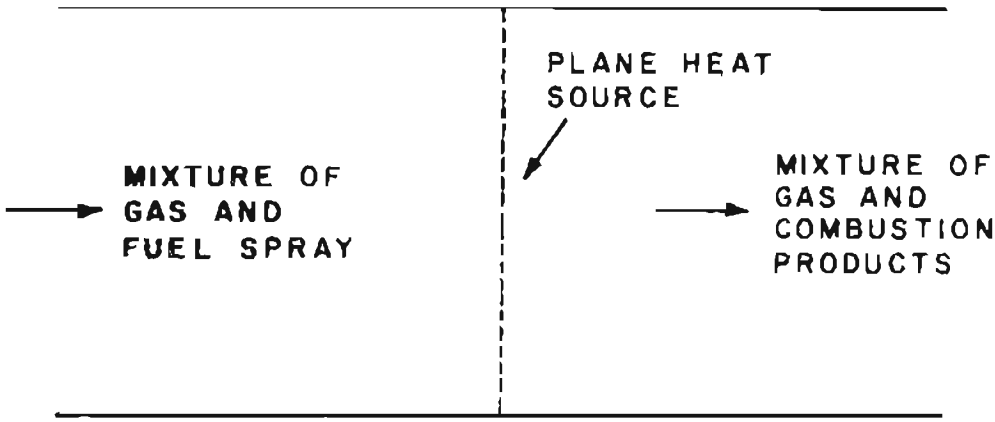

FIGURE 1. SCHEMATIC DIAGRAM OF FUEL SPRAY AND PLANE HEAT SOURCE

5. For the small relative velocities considered here, the droplets do not deform or shatter but are influenced by aerodynamic drag forces.

6. The droplet evaporation rate follows stagnant film relationships for pre- and post-ignition vaporization, corrected for forced convection.

7. Droplet ignition occurs when the liquid temperature reaches the level necessary for the formation of a stoichiometric fuel-air mixture at the liquid surface. According to reference 15 for hydrocarbon fuels this occurs when the liquid temperature, T_ℓ, is given by:

$$T_\ell = 0.74\ T_B - 70\ [^oC] \qquad (1)$$

where T_B is the liquid boiling point. Reference 15 suggests that for sufficiently high ambient air temperatures equation (1) results in a reasonable approximation of the ignition delay period. Before ignition the droplets act as sources of fuel vapor for the ambient gas. After ignition occurs, the consumption of fuel and oxidizer and the generation of products of combustion around the droplets follow the stoichiometry of fuel combustion.

Previous calculations (4) employed a prescribed gas temperature as the ignition criterion, regardless of the previous history of the droplets. The use of a prescribed ignition temperature simplifies the description of the transient droplet behavior through the ignition point, but underestimates the ignition delay for the droplets. Results were, therefore, presented (4) for various ignition temperatures, which is equivalent to changing the ignition delay time. The use of equation (1) as the ignition criterion implies a dependence on droplet size, since the time for reaching T_ℓ depends on the droplet diameter. However, T_ℓ does not depend on the ambient oxygen concentration. This, however, does not limit the usefulness of the results with respect to dilute sprays involved in aircraft crashes.

8. The equations describing the gas flow are written in terms of four species: fuel, oxidizer, products, and neutrals. They include the effects of conduction heat transfer and diffusion of species and are coupled to the liquid phase equations through appropriate source, or sink, terms for energy and mass transport. Chemical reactions for the fuel vapor, which is added to the homogeneous gas phase during the droplet pre-ignition vaporization period, are described in terms of one second order rate controlling step. The necessary chemical kinetic parameters are adjusted to give agreement with available experimental data.

9. Physical properties are computed for each downstream position and depend on the local gas phase temperature and concentration.

10. Boundary conditions include (a) the upstream temperature, velocity, and combustion of the spray, and (b) the downstream absence of any fuel as liquid or vapor. It is also necessary to specify the intensity and position of the plane heat source.

11. Turbulent sprays are described in terms of an eddy diffusivity model as in reference 13. Although this model does not represent the physical processes occurring in wrinkled flames, when the scale of turbulence is larger than the flame front thickness, it at least gives a reasonable qualitative variation of the effects of turbulence on the burning velocity. It is also assumed that there is no effect of the flame on the scale and intensity of turbulence.

LIQUID PHASE EQUATIONS.

a. Droplet flux balance:

$$N_j u_j = N_{jo} u_{jo} \tag{2}$$

where N_j is the number density of droplet group j which is moving with a velocity u_j, j = 1, ...n. n is the number of droplet groups at the upstream boundary which is denoted by the subscript $_o$.

b. Droplet momentum balance:

$$u_j \frac{du_j}{dx} = \frac{3}{8} \frac{\rho_g}{\rho_\ell} \frac{(v-u_j)}{R_j} |v-u_j| \, C_{Dj} \tag{3}$$

The drag coefficient is $C_{Dj} = 27/Re_j^{0.8}$, (Reference 16). v is the gas speed, R_j is the radius of droplet group j, $Re_j = 2R_j|v-u_j|/\nu$ is the Reynolds number, and ρ_g and ρ_ℓ are the gas liquid phase densities, respectively. ρ_ℓ is assumed to be constant.

c. Droplet energy balance:

$$Zh_j \, (T-T_j) = -\frac{dR_j}{dt} \rho_\ell \, L + C_{p\ell} \, \rho_\ell \, R_j \, \frac{1}{3} \frac{dT_j}{dt} \tag{4}$$

The heat transfer coefficient h_j is given by the relationship of Ranz et al (17):

$$\frac{2R_j h_j}{k} = 2 + 0.6 Re_j^{0.5} \tag{5}$$

where k is the thermal conductivity of the gas. T_j is the droplet temperature, which is assumed uniform within the drop. L is the heat of vaporization and $c_{p\ell}$ is the heat capacity of the fuel, which is assumed to be constant. Z is a correction factor for using equation (5) with droplets where vaporization is appreciable. It is the ratio of the droplet heat transfer coefficient with vaporization to that with negligible vaporization. It is given by (reference 16)

$$Z = \frac{z}{\exp(z)-1} \tag{6}$$

where

$$z = -2R_j \frac{dR_j}{dt} \frac{c_{pf}\rho_\ell}{k \, Nu_j} \tag{7}$$

d. Droplet evaporation rate:

The following equation was used for the rate of radius change of burning droplets (8):

$$\frac{dR_j}{dt} = -\frac{k}{R_j c_p} \ln \left[1 + \frac{c_p(T-T_j)}{L} \quad \frac{QY_0}{\alpha_0 L} \right] \tag{8}$$

where Q is the heat of reaction for the fuel, Y_0 is the local oxidizer mass fraction, α_0 is the stoichiometric coefficient for the oxidizer, and c_p is the local value of specific heat for the gas. For quasi-steady state evaporation without burning, equation (8) was used without the term $(QY_0/\alpha_0 L)$, provided the droplet temperature was near the liquid fuel boiling point. The initial transient preheat and vaporization period was described by the following relationship (18):

$$\frac{dR_j}{dt} = \frac{k}{c_p \rho_\ell} \frac{(Nu_j Z)}{2R_j} \left[\frac{Y_{Fj} - Y_F}{1 - Y_{Fj}} \right] \tag{9}$$

where it is assumed that the heat and mass transfer processes around a droplet are similar. The fuel mass fraction at the droplet surface, Y_{Fj}, is given by the Clapeyron equation:

$$Y_{Fj} = \frac{M_F}{M} \exp \left[\frac{LM}{R} \left(\frac{1}{T_B} - \frac{1}{T_j} \right) \right] \tag{10}$$

e. Spray evaporation rate:

$$\dot{m} = -\sum_j N_j \rho_\ell 4\pi R_j^2 \frac{dR_j}{dt} \tag{11}$$

where $\dot{m}$ is the spray evaporation rate.

f. Spray enthalpy flux:

$$\dot{H}_s = \sum_j N_j u_j \rho_\ell 4\pi R_j^2 \frac{dR_j}{dt} \left[\int_{T_r}^{T_j} c_{p\ell} dT + H^o_{F\ell} \right] \tag{12}$$

where $\dot{H}_s$ is the spray enthalpy flux, and H^o_F is the standard enthalpy of formation for the liquid fuel taken at temperature T_r.

Equations (11) and (12) together with the expression for spray volume:

$$V_s = \sum_j N_j \frac{4\pi}{3} R_j^3 \tag{13}$$

provide the necessary coupling terms between the liquid and the gas phase.

GAS PHASE EQUATIONS.

For constant pressure and low speed flow of a dilute spray the momentum equation for the gas flow can be neglected. The remaining equations for the gas are as follows:

a. Global continuity:

$$\rho_g u + \sum_j N_j u_j \rho_\ell \frac{4\pi}{3} R_j^3 = \dot{M} \tag{14}$$

where $\dot{M} = \rho_{go} u_o + \sum_j N_{jo} u_{jo} \rho_\ell$ is the mass flux for the mixture.

b. Species conservation:

$$\frac{d}{dx}(\rho_g v Y_i) - \frac{d}{dx}\left(\rho_g D_i \frac{dY_i}{dx}\right) = w_i + \dot{m} f_i \tag{15}$$

$$i = F, O, P, N$$

where Y_i is the mass fraction for species i, and D_i is the binary diffusion coefficient for the ith species. The term $\dot{m} f_i$ in equation (15) refers to the volumetric rate of species produced or consumed within the boundary layer of the droplets in the spray. Before ignition $f_i = \delta_{Fi}$, where δ_{Fi} is Kroenecker's delta. After ignition $f_F = 0$, and $f_i = \alpha_i$, i = O, P. The reaction term w_i is given by the Arrhenius expression:

$$w_i = \alpha_i B \rho_g^2 Y_F Y_o \exp(-E/\overline{R}T) \tag{16}$$

where E is the activation energy and $\overline{R}$ the gas constant. B is a frequency term and depends on temperature according to $B = B_o T^{\frac{1}{2}}$, where B_o is a constant. Using equation (14), equation (15) can be rewritten as follows:

$$\rho_g v \frac{dY_i}{dx} - \frac{d}{dx} \rho_g D_i \frac{dY_i}{dx} = w_i + \dot{m}(f_i - Y_i) \tag{17}$$

c. Energy conservation:

$$\rho_g v H_g - k \frac{dT}{dx} + \dot{H}_s = \text{constant} \tag{18}$$

where H_g is the gas enthalpy. H_g is given by the following equation:

$$H_g = \sum_i Y_i \int_{T_r}^{T} c_{pi} dT + H_i^o \tag{19}$$

where H_i^o is the standard enthalpy of formation for the gas at T_r and c_{pi} is the specific heat of species i. Using equation (19), equation (18) can be rewritten as follows:

$$\rho_g v H_g - \frac{k}{c_p}\frac{dH_g}{dx} + \dot{H}_s = \Psi \tag{20}$$

where c_p is the gas specific heat. The constant Ψ in equation (20) is evaluated at the downstream boundary where the derivative with respect to x is assumed to be zero. The addition of heat to the mixture is accomplished by changing the value of this constant at the position of the heat source, by an amount equal to the added heat flux.

d. Equation of state:

$$\rho = pM/[(1-V_s)\overline{RT}] \tag{21}$$

where V_s is the spray volume (equation 13) and M is the molecular weight of the mixture:

$$M = \sum_i 1/(Y_i/M_i) \tag{22}$$

BOUNDARY CONDITIONS.

a. Upstream boundary conditions at $x = 0$ require a complete specification of the mixture in terms of temperature, speed, gas composition and droplet number density. For the present work the spray was polydisperse, the gas was air, and there was velocity equilibrium between the droplets and the gas. Equation (9) results in a non-zero droplet evaporation rate at the upstream boundary. Results were, therefore, obtained for a fixed distance between the upstream boundary and the plane heat source.

b. Downstream boundary conditions are expressed in terms of vanishing gradients for all variables involved. Thus, at $x = x_L$ it is required that $dY_i/dx = 0$ and $dH_g/dx = 0$, which implies the absence of liquid phase, or $N_i = 0$.

PROPERTY CALCULATIONS.

Properties were computed using the local gas temperature and mixture concentration. It is assumed that for dilute sprays the Lewis number $(\rho c_p D/k)$ can be set equal to one. The properties under consideration are, therefore, k, D_i, μ and c_p. Following reference (19) for the molecular values of k

$$k = \sum_i n_i k_i \tag{23}$$

and

$$\mu = \sum_k n_i \mu_i \tag{24}$$

where n_i is the mole fraction of species i, while k_i and $_i$ are the molecular thermal conductivity and viscosity of the species. The specific heat is given by:

$$c_p = \sum_i Y_i c_{pi} \tag{25}$$

Following reference (20) the individual species properties were expressed as linear functions of temperature.

For turbulent sprays the computed laminar transport coefficients k and D were augmented using the following relationships (13):

$$k_t = k + \rho c_p \varepsilon \tag{26}$$

and

$$D_{it} = D_i + \varepsilon \tag{27}$$

where k_t and D_{it} are the turbulent thermal conductivity and species diffusion coefficients, respectively, and ε is the eddy diffusivity. In turn:

$$\varepsilon = \lambda u' \tag{28}$$

where λ is a characteristic turbulent length scale of the approach flow and u' is the rms velocity fluctuation.

In the formulation described above, the burning velocity is not an eigenvalue. It is, instead, defined as the lowest upstream gas velocity for which the boundary conditions of the problem can be maintained. This is equivalent to calculating incipient "flashback" conditions for a liquid fuel spray streaming towards a hot source; for example, towards a region where burning of combustible material is already taking place.

NUMERICAL CALCULATION

Equations (3) and (4) and either (8) or (9) for a single droplet can be easily integrated using a step-by-step method beginning at the upstream boundary, provided that the gas profiles are known. In turn, equations (14), (17), and (20) and the boundary conditions for the gas, form a two point boundary value problem of first and second order non-linear ordinary differential equations, which require the spray coupling terms given by equations (11) through (13) for their integration. Following Williams' (6) suggestion, the following iterative scheme was used for the solution of the coupled set of spray and gas phase equations: beginning with assumed gas profiles, the equations for each droplet group were solved, and the coupling terms calculated. The coupling terms were then used in the solutions of the gas phase equations, thus providing profiles for new spray phase calculations, and so on. Convergence was achieved when there were negligible changes in the coupling terms between iterations:

$$S = \sum_m \left[\Delta(\dot{m}_m)^2 + \Delta(\dot{H}_{sm})^2 + \Delta(V_{sm})^2\right] \leq e \tag{29}$$

where the summation is taken over all grid points, m, Δ denotes differences between successive iterations, and e is a small positive number. The concentrations of species at the downstream boundary were checked for agreement with those calculated using the stoichiometry of fuel burning.

Regarding the details of the numerical integration, the first order differential equations for the spray (Equations 3, 4, and 8 or 9) were integrated beginning at x = 0 using Euler's predictor-corrector method. The gas phase species conservation equations are non-linear through the temperature and concentration dependent gas properties, but the main contribution

to non-linearity arises from the reaction term w_i in the species equations. Using the quasi-linearization method described by Fay et al (21), solution of equation (17) for i = F, O, and P was therefore approached through successive iterations involving a linearized form of w_i and its derivatives. The round-robin iteration scheme involved successive calculation of product, fuel, oxidizer and enthalpy profiles, in that order, using the results of each previous iteration for computing non-linear terms, until the non-linear species equation (16) was very nearly satisfied. The matrices involved in the integration of the gas phase equations are tri-diagonal and can be easily inverted. The matrix inversion process was started at $x = x_L$, and required a Raphson-Newton iteration scheme for matching with the upstream gas boundary conditions.

For a given spray, numerical solution of the equations could be obtained provided the upstream gas velocity was larger than the burning velocity. Decreasing the velocity eventually results in non-converging iterations with relatively large values of e (Eq. 29). Moreover, the temperature calculated during each iteration became progressively larger in the upstream direction. Therefore, the criterion for a non-converging solution was the calculation of a temperature exceeding the droplet ignition temperature at a convenient upstream point. The value of burning velocity was bracketed between adjacent gas velocity values corresponding to convergent and non-convergent solutions. With slight modifications the integration method was also used to compute the burning velocity in a premixed gas without a liquid phase. This was accomplished by setting the droplet number density equal to zero, and adjusting the upstream value of fuel mass fraction for the desired fuel concentration.

The calculations were carried out using the IBM 360-67 computer at Rutgers University. The CPU time depended on the fuel concentration and droplet radius, but averaged about three minutes for a convergent solution, and about five minutes to determine lack of convergence. For a given fuel concentration, decreasing the droplet radius results in a decrease in burning time of the spray. Consequently, sprays with very small droplets required a minute step size, Δx, and long computing times. For a monodisperse spray with an 8μm diameter droplets the CPU time for a convergent solution was approximately 20 minutes. Bracketing of the flame propagation velocities was accurate to ±5%.

Calculations were carried out for monodisperse tetralin-air sprays (4), and polydisperse kerosene-air sprays. Thermodynamic properties of liquid tetralin were obtained from the Handbook of Chemistry and Physics (22). Table I lists pertinent physicochemical properties of kerosene that were used in the calculations. The properties of fuel vapor were assumed to be those of decane and were obtained from correlations used by Faeth et al (20).

The heat source intensity was sufficient to increase the pure air stream temperature by approximately 1200°K. The computed burning velocities were insensitive to the choice of heat source intensity, provided the resulting temperature was sufficiently high for consumption of fuel vapor.

TABLE I. PROPERTIES OF KEROSENE

Density:	0.8 gm/cm^3
Heat Capacity:	0.64 cal/gm^oK
Latent Heat of Vaporization:	61 cal/gm
Heat of Formation (liquid):	598 cal/gm
Heat of Reaction:	10,400 cal/gm
Chemical Formula:	$C_{12}H_{26}$
Stoichiometric Coefficient for Oxygen:	3.48
Stoichiometric Coefficient for Products:	4.48
Physical Properties of the Vapor and the Products of Combustion:	Decane Vapor (20)
Boiling Point:	483^oK

FAA WJH Technical Center
00090601

For the calculations reported in this work $v_o = u_{jo}$ and $T_o = T_{jo}$ except as noted. The step size was between 0.5×10^{-3} and 5×10^{-3}cm, and the integration region extended 0.2 to 0.5 cm upstream from the heat source, and 0.2 cm to 0.5 cm in the downstream direction depending on the droplet size.

RESULTS AND DISCUSSION.

RESULTS OBTAINED USING A PRESCRIBED GAS TEMPERATURE AS THE IGNITION CRITERION OF THE LIQUID DROPLETS. A discussion of calculated burning velocities of laminar tetralin-air sprays is found in reference 4. These were obtained using various prescribed gas temperatures as the conditions for ignition of the liquid droplets and as a result the ignition delay of the droplets is underestimated. The present report contains additional results obtained using the ignition criterion described by equation (1). The new results are qualitatively similar to those of reference 4, but more realistic since the ignition delay period of the droplets is taken into account.

CHOICE OF THE PARAMETERS B_o AND E FOR FUEL VAPOR-AIR MIXTURES. Published experimental data on premixed flame burning velocities was used for obtaining appropriate values of the pre-exponential factor, B_o, and the activation energy, E, which are necessary for describing the homogeneous gas phase reactions in the spray model. This was accomplished by matching available experimental laminar burning velocities with calculated results using assumed pairs of B_o and E. Reference 23 gives a value of 40 cm/sec for the maximum laminar burning velocity of a kerosene vapor-air mixture at an equivalence ratio* of 1.06. Figure 2 shows computed burning velocities which were obtained using $B_o = 4 \times 10^{12}\text{sec}^{-1}$ and E = 40,000K cal/gmole The experimental point at 40 cm/sec (23) is in good agreement with the calculated results. Similar results were obtained for tetralin-air vapor mixtures, and resulted in $B_o = 5 \times 10^{12}\text{cm}^{-1}$, and E = 40,000 cal/gmole. The present value of B_o is different than that employed in reference 4 because the experimental data that was used for the matching process in the previous work was actually spray data with 8μm diameter droplets, which did not accurately represent the fuel vapor behavior.

MONODISPERSE TETRALIN-AIR SPRAYS. Figure 3 shows the effect of fuel concentration on the calculated laminar burning velocity of monodisperse tetralin-air sprays with 15 m diameter droplets. On the same Figure are included calculated results from reference 4 for various values of the prescribed gas temperature for droplet ignition, T_I, for comparison with the present results which were obtained using equation (1) as the ignition criterion for the liquid droplets. Both methods of describing the conditions of droplet ignition yield a qualitatively similar dependence of burning velocity on fuel concentration. However, the use of equation (1) seems

*The equivalence ratio is defined as the ratio of the actual over the stoichiometric fuel-air ratio.

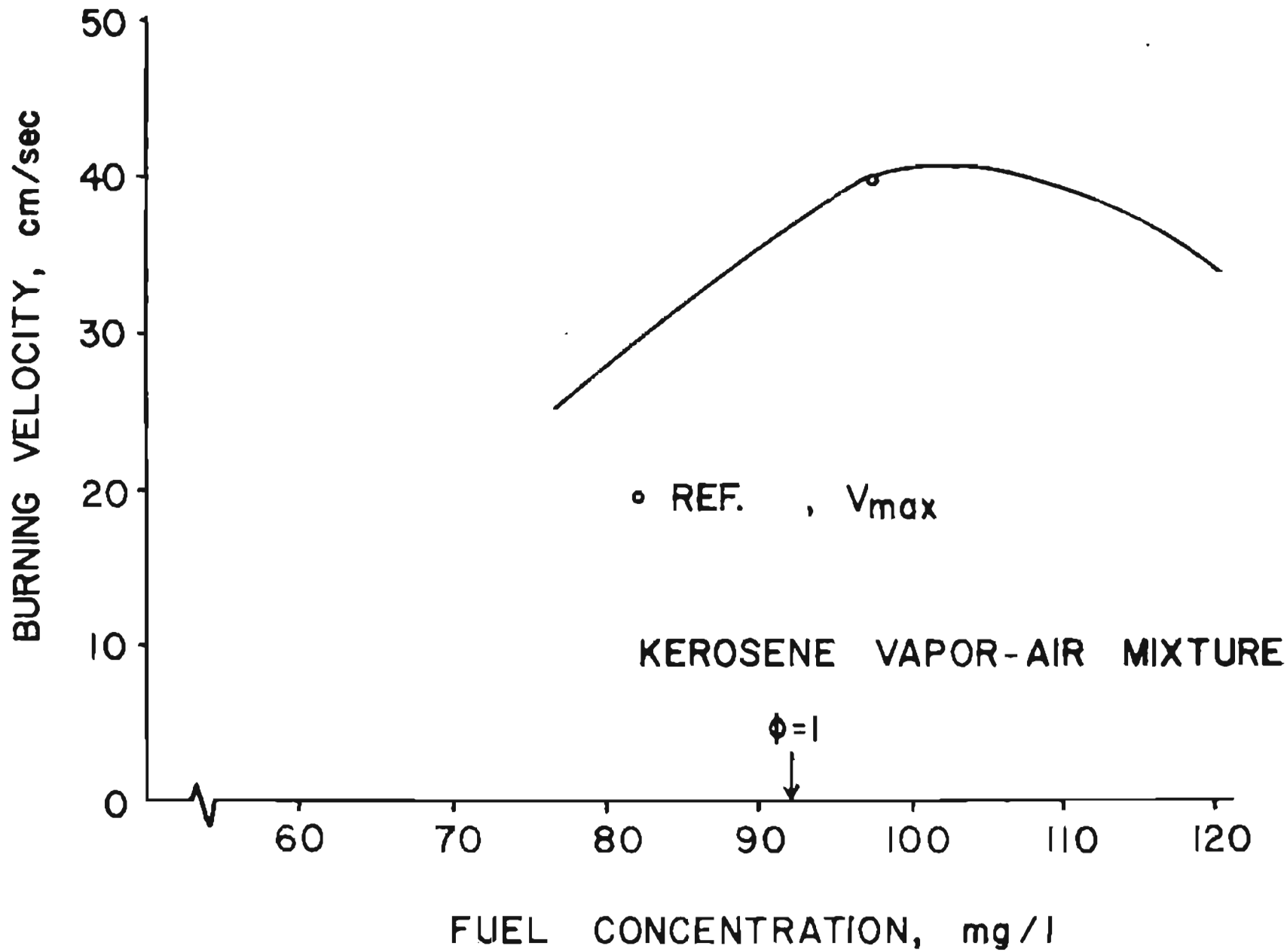

FIGURE 2. BURNING VELOCITIES OF KEROSENE VAPOR-AIR MIXTURES

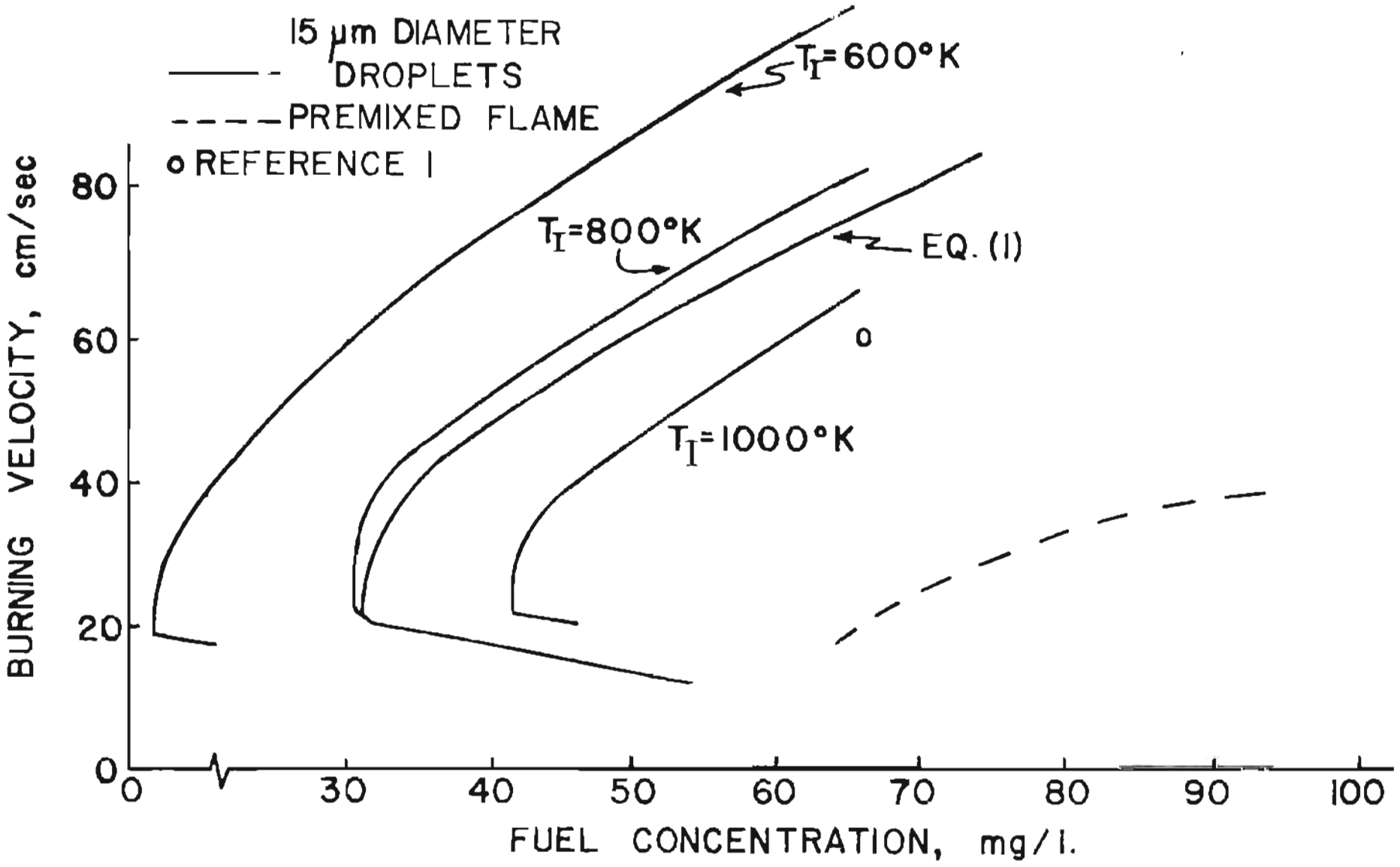

FIGURE 3. BURNING VELOCITY VS. FUEL CONCENTRATION FOR MONODISPERSE TETRALIN-AIR SPRAYS. DROPLET DIAMETER IS 15μm

to be more convenient because it does not require the use of T_1 as an input to the calculations. In addition, it results in a burning velocity of 76 cm/sec at a fuel concentration of 69 mg/l which is in reasonable agreement with the experimental point of reference 1, also shown on Figure 3.

Calculated burning velocities for a premixed gas are also shown on the same figure, and are lower than those in the mist with equivalent fuel concentration. For relatively low fuel concentrations Figure 3 shows that it is possible to have two different speeds of flame propagation in a spray. The higher upper branch of the curve is associated with heterogeneous combustion around the droplets with very little preignition vaporization. The lower branch of the curve describes the mist as it moves very slowly towards the flame, and there is appreciable time for preignition vaporization. Since the pure vapor has a lower burning velocity than the 15μm mist, the effect of preignition vaporization is a double valued burning velocity at the same fuel concentration. Similar behavior can be shown for large droplets. However, as the droplet size increases at fixed fuel concentration, appreciable preignition vaporization in a spray occurs for speeds which are too low to be of practical significance.

Figure 4 shows the effect of droplet diameter on the laminar burning velocity of tetralin-air sprays of fixed fuel concentration at 69 mg/l. Beginning with sprays of large droplets, decreasing the diameter results in increasing the burning velocity, since the burning rate of a monodisperse fuel spray with constant initial fuel concentration is inversely proportional to the square of the droplet radius. Eventually, as the droplet diameter becomes very small the droplets completely evaporate before reaching the ignition temperature of the liquid fuel, and the burning velocity approaches that of a premixed gas. For small droplets the final decrease in burning velocity as the droplet diameter decreases is, therefore, due to the transition from a heterogeneous to a premixed gas burning mechanism. Thus the curve on Figure 4 has a maximum at a droplet diameter between 0 to 15μm. At zero diameter the burning velocity is that of a premixed gas.

It should be noted that the calculated burning velocity at 8μm droplet diameter, which is shown on Figure 4, corresponds to flame propagation with appreciable liquid preignition vaporization or to the lower branch of a curve similar to that shown on Figure 3 for 15μm diameter droplets. The second higher burning velocity solution, which corresponds to the upper branch of the curve, results in a burning velocity of 120 cm/sec. The use of the lower branch solution is justified because of agreement with previous experimental data as will be shown in the next section. Rigorous justification for this choice will have to await further study.

The following section presents experimental data which confirm the influence of droplet diameter on burning velocity which is predicted by results such as those shown on Figure 4. A qualitative discussion of possible mechanisms for flame propagation in a spray will also be discussed in that section.

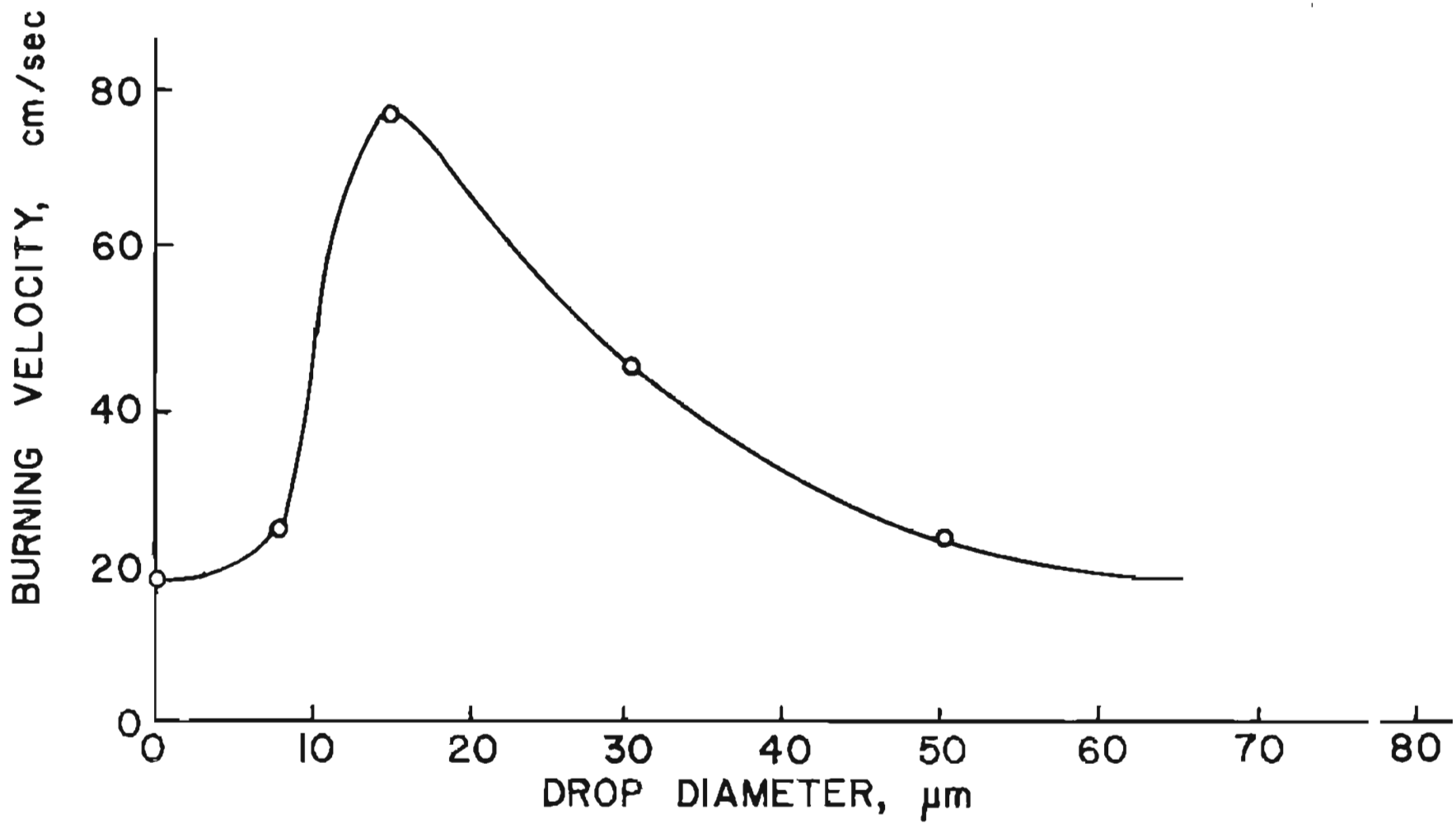

FIGURE 4. DROP DIAMETER VS. BURNING VELOCITY FOR MONODISPERSE TETRALIN-AIR SPRAYS. FUEL CONCENTRATION IS 69 mg/l

COMPARISON OF CALCULATED BURNING VELOCITIES WITH AVAILABLE EXPERIMENTAL DATA. Table 2 can be used for comparing burning velocities with presently available experimental data. The experimental measurements are those of Burgoyne and Cohen (1) for monodisperse tetralin sprays, as well as one point obtained during the present work using turbulent polydisperse kerosene-air sprays. For the turbulent flow calculations the upstream turbulent intensity was 8%, and the turbulence scale was 0.3 cm. There were equal to the experimentally measured turbulence intensity and the O.D. of the pilot flame tube, respectively. Agreement between predicted and measured values for tetralin is satisfactory except for the relatively large droplet diameter of reference 1. It should be noted that for droplets larger than approximately 20μm, the experimental procedure of reference 1 consisted in measuring the mean burning velocity using direct photographs of highly asymmetric flames anchored at the mouth of a tube. For droplets smaller than 20μm, the flame had a well-defined flame cone, and could be photographed using a shadowgraph method.

EXPERIMENTAL WORK

PREVIOUS WORK ON THE EFFECT OF DROPLET SIZE ON THE BURNING VELOCITY OF LIQUID-AIR SPRAYS.

The effect of droplet size on the burning velocity of liquid fuel sprays has been studied by several investigators to date. The experiments of Burgoyne and Cohen (1) using monodisperse tetralin-air sprays showed that the laminar burning velocity in sprays with very small droplets is smaller than the burning velocity in comparable sprays of larger droplets. Moreover, very small droplets appear to vaporize completely upstream of the flame front, thus giving the flame a premixed gas flame appearance, while large drops burn in diffusion flames around the liquid phase, thus giving the flame a "brush" type appearance. Unfortunately, the air-fuel ratio in Burgoyne and Cohen's experiments was not constant over a wide range of droplet diameters for finding a critical diameter for maximum burning velocity at constant air-fuel ratio.

The following mechanism for flame propagation can be used to qualitatively interpret the experimental results: In sprays of large droplets the flame propagation is in relatively vapor-free space with a relay process across the diffusion flames surrounding each droplet. Heterogeneous combustion around the droplets takes place in the optimum air-fuel ratio, and the droplets act as high temperature heat sources for the ignition of adjacent droplets, thus resulting in flame propagation with pockets of cool air remaining between the droplets. In addition, the thermal expansion of the gas around the burning droplets intensifies the transport process, and accelerates the burning velocity. At constant air-fuel ratio, beginning with relatively large droplets, an initial reduction in a droplet size results in a more closely spaced suspension, a higher volumetric heat release rate, and consequently an increase in burning velocity. However, further decrease in droplet size eventually results in significant amounts of fuel evaporating ahead of the flame and mixing with the air between the droplets.

TABLE 2. CALCULATED VS. EXPERIMENTAL BURNING VELOCITIES

Flow	Fuel	Drop Diameter (μm)	Mass Concentration (mg/l)	Burning Velocity Experimental (cm/sec)	Burning Velocity Calculated (cm/sec)
laminar	Tetralin	15	69	59	76
laminar	Tetralin	22	64	55	42
laminar	Tetralin	30	60	67	35
laminar	Tetralin	38	48	58	23
Turbulent	Kerosene	Polydisperse Spray A	69	60	67

Burning of this lean homogeneous fuel-air mixture requires high temperatures, or a relatively large amount of heat transferred ahead of the flame for ignition. As a result, for the relay flame transfer associated with heterogeneous combustion around the droplets, an increase in the amount of fuel evaporated before ignition will also decelerate the burning velocity. Thus, increasing the droplet size in such a spray may result in increasing the burning velocity. Although this was not confirmed by previous experimental investigations, an interesting conclusion of the previous results is that there is a range of droplet diameters for maximum burning velocity in a spray, and that very find atomization may not always be desirable in combustion applications.

A quantitative interpretation of the transition from heterogeneous to homogeneous combustion in a spray, and of the accompanying influence on burning velocity, must take into account the relative magnitudes of the characteristic ignition delay and burning times for individual droplets and for a premixed gas. According to Williams' (6) approximate analysis, it is expected to have both increases and decreases in burning velocity upon transition from heterogeneous to homogeneous combustion in a spray depending on the properties of different fuel oxidizer systems. Reference 4, using several different ignition delay times for the droplets, shows how this transition process can result in a maximum value for the calculated burning velocity as the droplet diameter decreases at constant air-fuel ratio. References 24 and 25 include discussions of a possible decrease in air-fuel ratio as the spray particle size decreases in the lean limit for flame propagation.

Mizutani and Nakajima(10) used an open inverted-cone-flame burner, and measured the local rate of flame spread in turbulent kerosene-mist-propane-air mixtures. The normal rate of flame spread, S_u, into the mixture was defined in terms of the expression $S_u = \overline{V} \sin \overline{\theta}$, where $\overline{V}$ is the local mean flow speed and $\overline{\theta}$ is the angle between the mean position of the flame front and of tracks from every small droplet in the flow. Since droplets track the flow streamlines according to their size, it is not clear why it is appropriate to use tracks from small droplets for the measurement of $\overline{\theta}$ in polydisperse sprays.

The measurements in reference (10) were carried out in a region of relatively constant average gas speed and turbulence intensity. It is, therefore, assumed that flame elements reach their "equilibrium" speed of propagation in that region so that the measured value of S_u is the burning velocity of the mixture. Data in reference (10) shows that for the same upstream conditions and overall air-fuel ratio, addition of kerosene spray to a propane-air flame increases the burning velocity while addition of kerosene mist consisting of very fine droplets may produce the opposite effect. It was concluded that the measured changes in burning velocity, as the kerosene is added in relatively large droplet or mist form, are a consequence of the presence of the mist, and not of the different physicochemical properties of kerosene and propane vapor. Thus, this conclusion is also in support of the previous qualitative description of the effect of droplet size on the burning velocity.

The present work is an experimental investigation of the effect of droplet size on the burning velocity of polydisperse kerosene-air sprays. The experiments were similar to those in reference (10), and the normal rate of flame spread into the combustible mixture, measured in a region of relatively constant mean flow speed and turbulent intensity, will be identified as the burning velocity of the mixture for the turbulence level present in the apparatus. No rigorous justification for this assumption is attempted here. However, from schlieren photographs it appears that the flame front is flat in that region, suggesting a constant speed of flame propagation.

EXPERIMENTAL APPARATUS AND PROCEDURE

The experimental apparatus was similar to that used in reference (10) and is shown schematically on Figure 5. It consisted of a vertical stainless steel tube 24 mm I.D. and 1 m long with kerosene-air spray flowing upwards and discharging into the ambient atmosphere. A small acetylene pilot flame, with a 3 mm O.D. burner, was located at the exit of the tube and was used to ignite the spray. The resulting inverted cone flame was photographed using a schlieren system. The primary air supply was metered using a rotometer, and a second rotometer was used for measuring the air supply to an ultrasonic atomizing nozzle operating at 35,000 cps which was employed for atomizing the liquid fuel. The fuel was supplied to the nozzle through a variable flow rate rotary pump, and the air-fuel ratio, as well as the droplet size distribution, were set by adjusting the pump exit pressure, and the primary and atomizing air flow rates. The air-fuel ratio was calculated from the rotometer readings, and by weighing the mixture collected at the tube exit using a plastic bag. The kerosene and air flow rates were constant for all the experimental runs, and the air-fuel ratio was 18.

Figure 6 shows the distribution along the tube radius of mean velocity and rms velocity fluctuations upstream from the flame front at the tube exit measured using hot wire anemometry. The flow Reynolds number based on the tube diameter was 2700. The rms fluctuations shown are average values including turbulent bursts due to the transitional flow regime.

Droplet diameters were measured from photographs of the spray obtained using an instantaneous light source with a flash duration of approximately 5μ sec. The optical system was similar to that used by Ingebo (26), and produced a magnification of X8 on the film with a depth of field of approximately 1 mm. To avoid excessive attenuation of the light passing through the fine spray, a 10 mm wide slit was placed perpendicular to the light beam over the tube exit when photographing the droplets. Photographs were taken only at one position corresponding to a distance of half a tube radius from the tube centerline and from the tube exit. Droplet sizes were measured after magnifying the negatives about 3 times. About 300-650 droplets were counted using several negatives for each run. The droplet sizes measured with this method are subject to uncertainty because of (a) personal interpretation of the position of the droplet boundaries, as well as of the droplets which are out of focus, and (b) the effect of film developing time on the image size of the very small droplets. The counting and film developing were carried out by the same person to minimize differences in interpretation and developing technique. The resulting droplet size counts were used to qualitatively describe the relative extent of atomization between different sprays. This was accomplished by comparing the liquid volume in

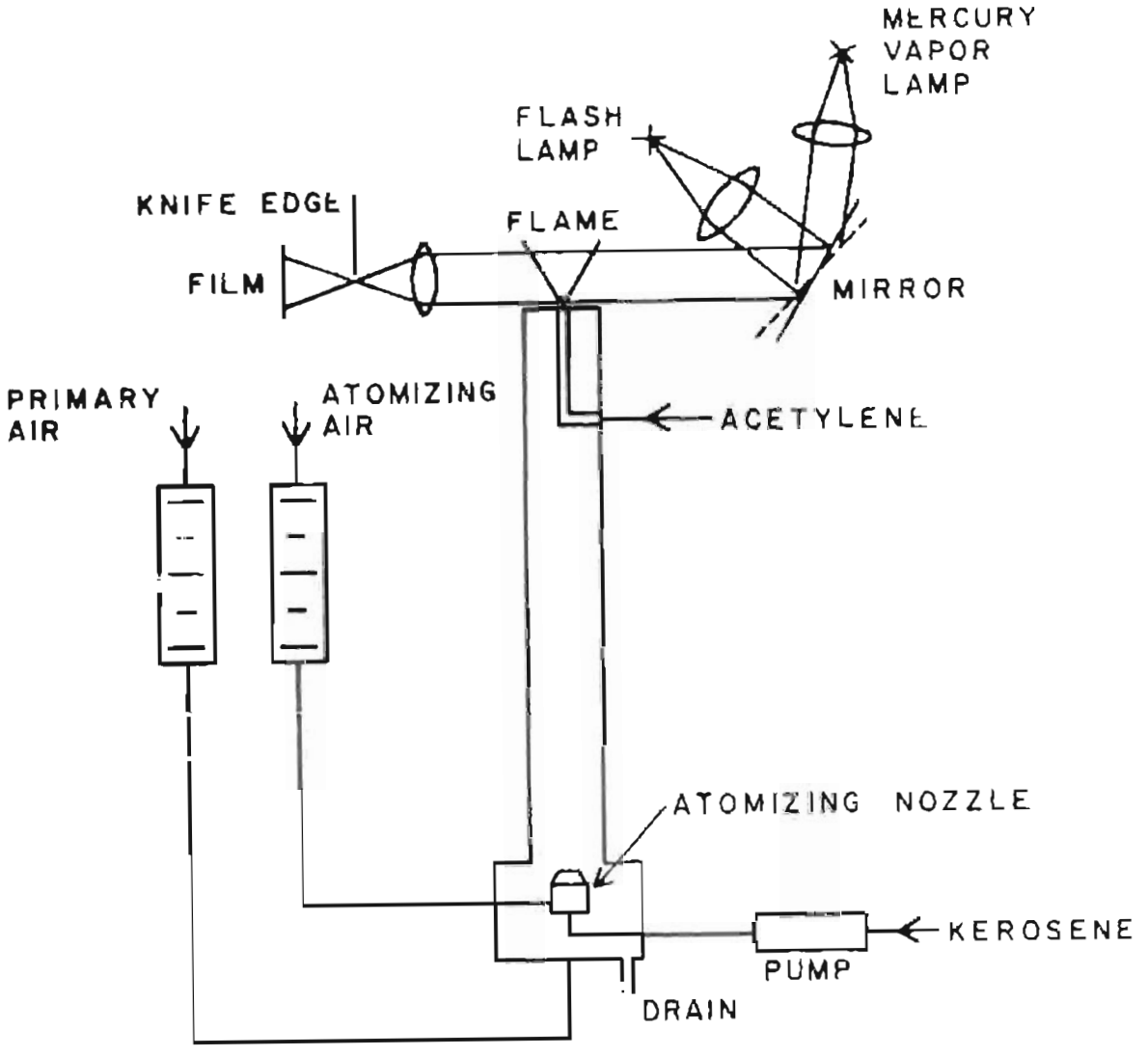

FIGURE 5. SCHEMATIC DIAGRAM OF THE EXPERIMENTAL APPARATUS

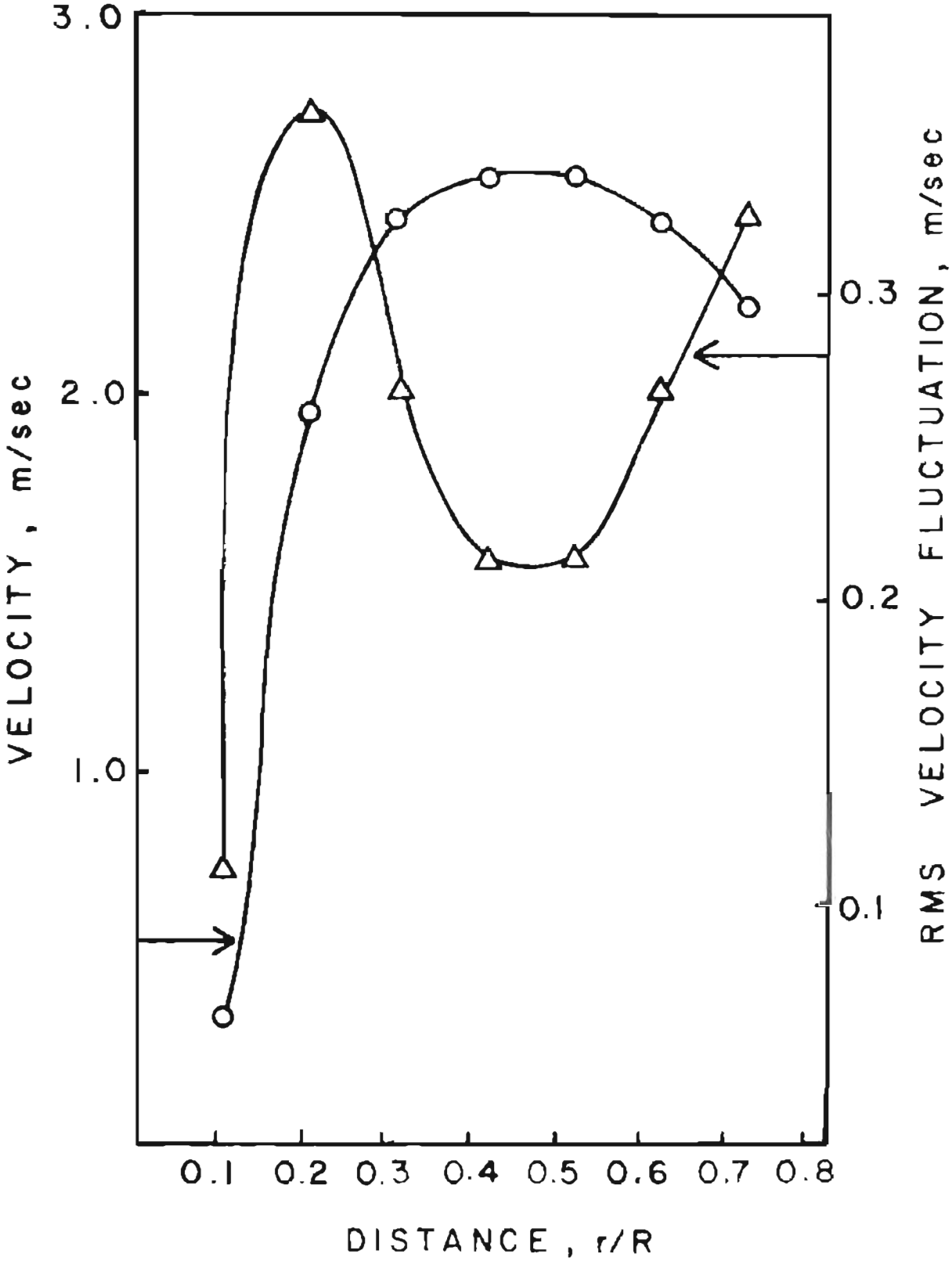

FIGURE 6. MEAN AIR VELOCITY AND RMS VELOCITY FLUCTUATIONS AT THE TUBE EXIT

each droplet size group for the sprays tested. Droplets that appeared smaller than 30μm in diameter were not included in the results because their diameters could not be measured accurately with the present system.

Figure 7 shows schlieren images of flames obtained for three different degrees of atomization. The exposure time was 1000^{-1} sec, the magnification was X3 on the film, and the depth of focus was about 6 mm. The light source was a high pressure mercury vapor lamp. Droplet streaklines can be clearly observed ahead of the flame using the photographic negatives, and can be used to track the mean position of particle paths in the flow. Occasional large scale turbulent bursts produced large scale distortions of the flame front, and only photographs where the flame front appeared smooth were used for measurements.

The burning velocity, S_u, was calculated using the relation $S_u = \bar{V} \frac{r_1}{r_2} \frac{\Delta r}{\Delta \ell}$ which is derived from the diagram on Figure 8. $\bar{V}$ is the mean flow velocity over a length Δr, measured at the tube exit and at a radial distance of half the tube radius, and $\Delta \ell$ is defined in terms of the surface enclosed by the mean particle path lines from Δr to the flame front. r_2 is the mean distance of $\Delta \ell$ from the tube centerline. It should be noted that $\Delta \ell$ appears as a straight line in the region of measurement. This method of calculating S_u minimizes the error due the differences in the mean position of streamlines and droplet path lines, since differences at large and small radii tend to cancel out. As it turned out this method of calculating S_u yielded values approximately 10% lower than those obtained by the angle method of reference (10).

RESULTS AND DISCUSSION

DEGREE OF ATOMIZATION IN THE SPRAYS TESTED. Figure 9 presents direct photographs of spray flames showing the effect of increasing fuel atomization on flame appearance. Figure 9a is for spray A consisting of relatively large droplets which burn enveloped in yellow diffusion flames. Combustion appears to take place downstream of a well-defined region that does not necessarily coincide with the flame front recorded on schlieren photographs. Increasing atomization in sprays C and E (Figures 9b and 9c) results in decreasing the number of individually burning drops, and in the gradual appearance of a blue flame front which is characteristic of premixed gas flames. Spray E is for the finest atomization that was used in the present tests and shows a well-defined blue flame front with a small number of burning drops in the downstream region.

Figure 10 shows the cumulative volume distribution versus droplet diameter for sprays A to E calculated from the droplet size counts. The liquid and air-flow rates were the same for all tests. As a result, the liquid volume in each size range was normalized with respect to the total volume of spray A. Spray A consisted of relatively large drops whose diameter could easily be measured. Figure 10 gives no information about the important droplet diameter range below 30μm. However, it shows that from spray A to spray E, (a) the number of large diameter droplets decreases, and (b) the fluid volume atomized in droplet diameters below 30μm increases. Thus, the results on Figure 10, together with the direct photographic observations of the spray flame, confirm that from spray A to spray E the atomization becomes progressively finer.

(a) SPRAY A

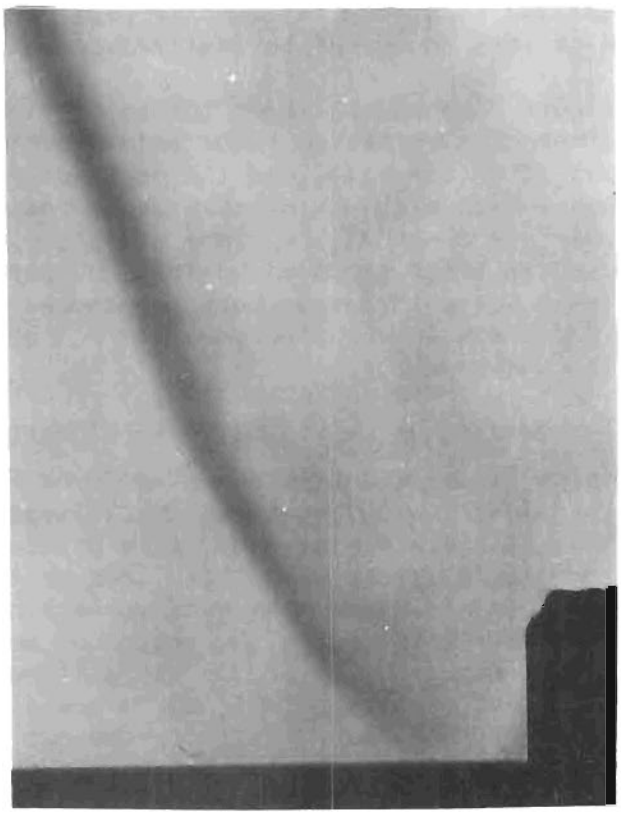

(b) SPRAY C

(c) SPRAY E

FIGURE 7. SCHLIEREN IMAGES OF FLAME FRONT

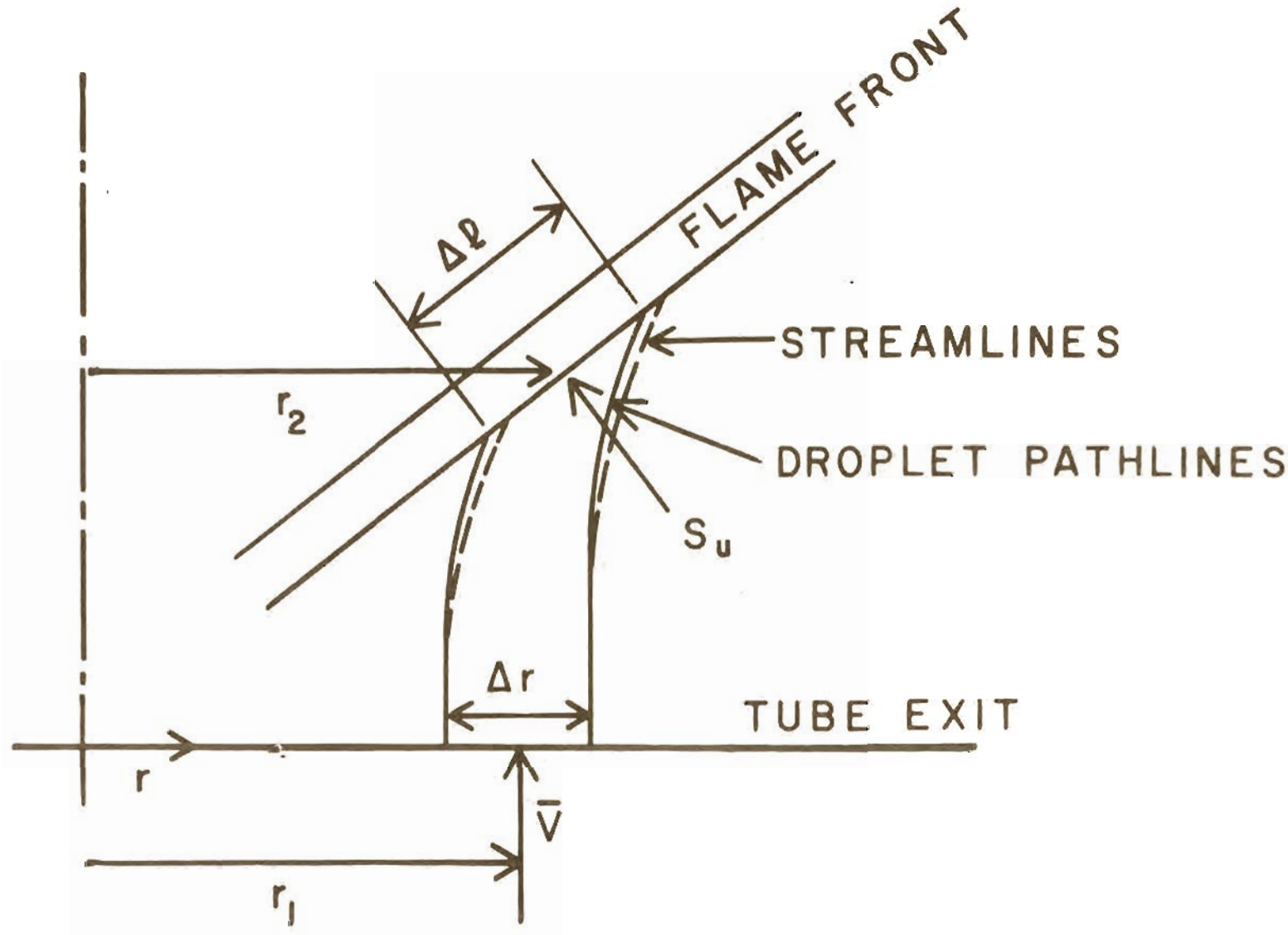

FIGURE 8. SCHEMATIC DIAGRAN USED FOR CALCULATING S_u

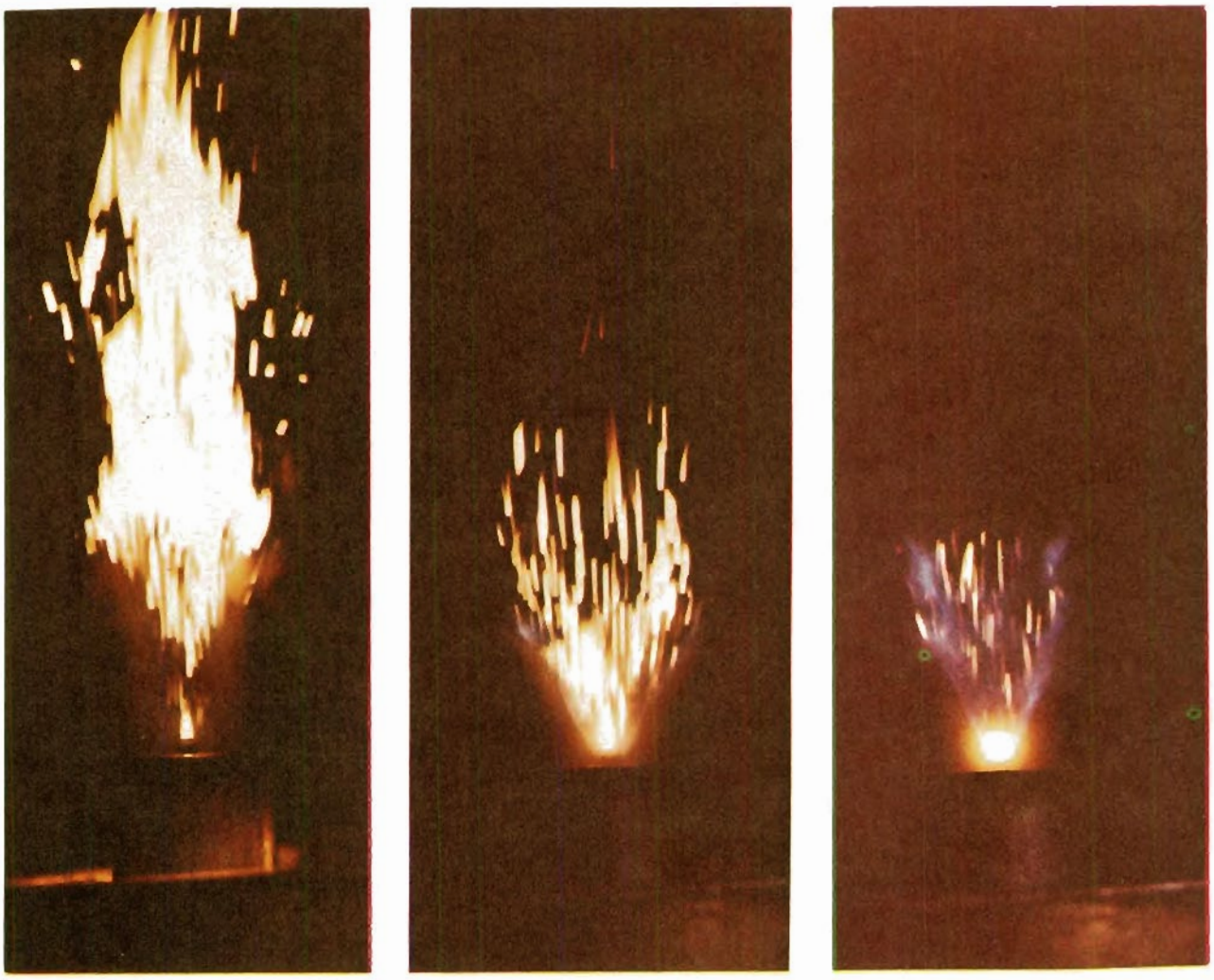

(a) SPRAY A (b) SPRAY C (c) SPRAY E

FIGURE 9. DIRECT PHOTOGRAPHS OF SPRAY FLAMES

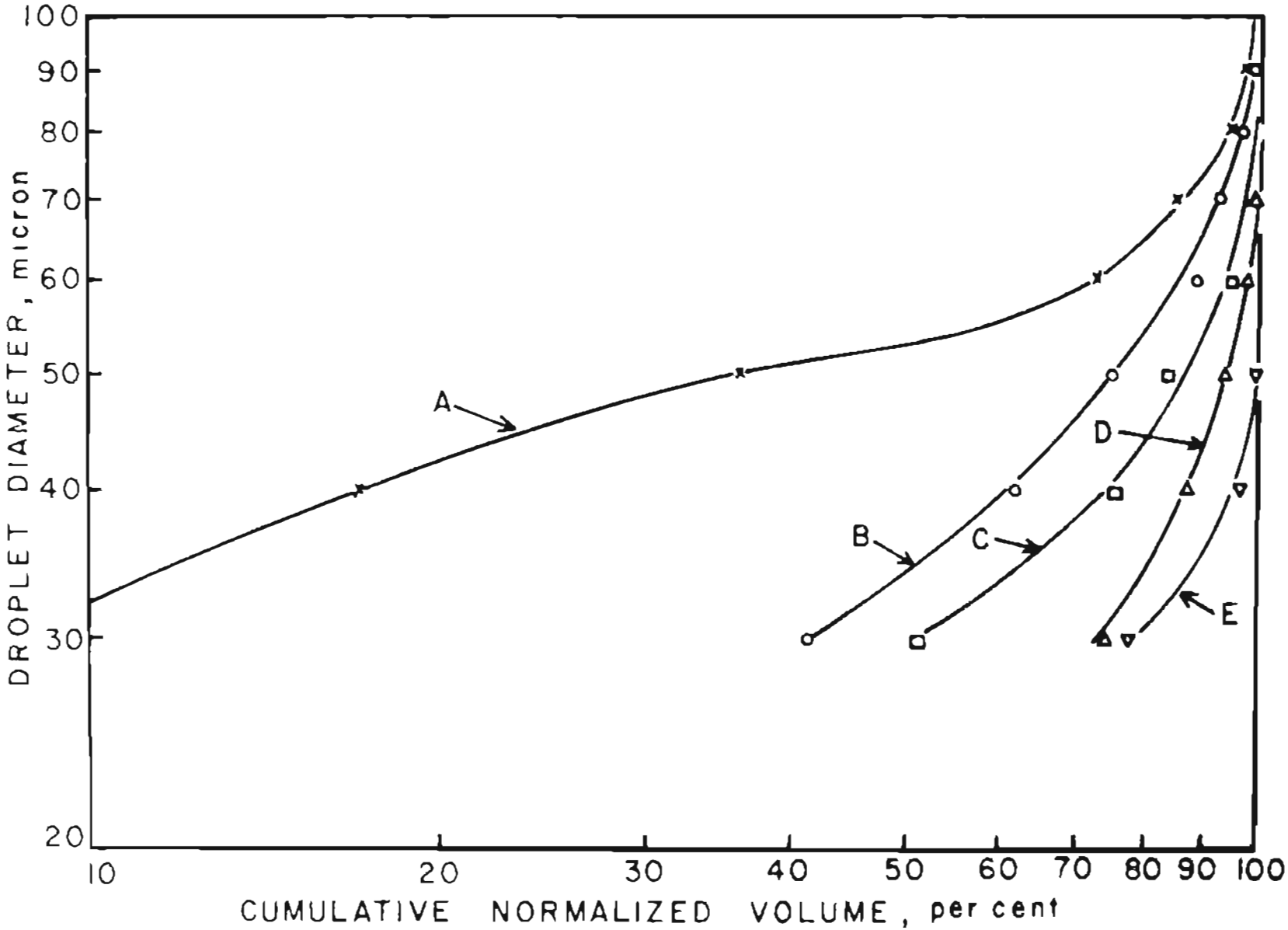

FIGURE 10. CUMULATIVE NORMALIZED VOLUME FOR THE SPRAYS TESTED

From the data it is possible to estimate the number density of the droplets in spray A, assuming a uniform spatial particle distribution. Table 3 shows the droplets counted per cm^2 of focal plane measured from photographic negatives, together with the calculated number density (droplets/cm^3) for each size group. The combined number density for spray A is thus estimated at 1750 droplets/cm^3. Using Table 3 and the liquid fuel density (0.8 gm/cm^3) it is possible to estimate the liquid concentrations at 6.8×10^{-5} gm/cm^3. This compares favorably with the value of 7.1×10^{-5} gm/cm^3 which is measured directly at the tube exit, and suggests that for spray A the measured particle size distribution includes practically all the droplets in that spray. Our inability to measure diameters below 30μm prevents us from making similar calculations for the other sprays tested.

BURNING VELOCITY RESULTS. Table 4 shows the burning velocities (S_u) measured for the sprays tested. The velocities are average values from several different measurements. It was estimated that measurements from photographic negatives resulted in a ± 4 cm/sec error in the calculated values of S_u. Reproducibility between different measurements was within ± 5 cm/sec from the average values of S_u shown on Table 4. S_u initially increased from 60 cm/sec for a relatively coarse spray to a maximum of 91 cm/sec as the degree of atomization increased. However, further atomization resulted in a decrease in burning velocity to 50 cm/sec for spray E, which for the present tests appeared to burn mostly as a premixed flame. It should be noted that the laminar burning velocity of kerosene vapor is reported as 40 cm/sec at an air-fuel ratio of 14 (23). From the results of Table 4 it appears that for a given kerosene-air mixture, there is a drop size distribution which results in a maximum rate of flame propagation, which is larger than that of a premixed gas of the same air-fuel ratio.

Observation of schlieren images of the flame front such as those on Figure 7 shows that as expected, the flame appears to be ignited in the boundary layer ahead of the pilot tube tip, and that the point of ignition is further upstream for spray C which had the maximum measured burning velocity. In addition, it should be noted that the angle of the flame with the vertical axis is not a true indication of burning velocity, because the effect of flow angle at the flame front must also be considered. Observation of the sample photographs on Figure 7 shows that the particle tracks appear to diverge outwards at the flame front by an increasing amount as the degree of atomization increases. This is because the zone of fuel burning (in gaseous or droplet form) downstream from the flame front is shortened as the droplet size decreases, thus increasing the effect of flame thrust, which is the reason for the diverging droplet pathlines at the flame front.

Reference 9 gives the following empirical correlation for the burning velocity of kerosene-air sprays in apparatus similar to that used in the present study:

$$S_u = \frac{6.800}{\bar{d}}(\phi - 0.012)\ (u')^{1.15}\ [\text{m/sec}] \qquad (30)$$

where ϕ is the fuel-air ratio, $\bar{d}$ is the Sauter mean diameter in microns, and u' is the rms velocity fluctuations in m/sec. For spray A and the

TABLE 3. DROPLET NUMBER DENSITIES FOR SPRAY A

Diameter Range, μm	Droplets/cm^2 (counted)	Droplets/cm^3
31 - 40	91	868
41 - 50	51	364
51 - 60	59	453
61 - 70	12	41
71 - 80	6	15
81 - 90	1	1
91 - 100	1	1
		1742

TABLE 4. BURNING VELOCITIES (AIR-FUEL RATIO = 18) KEROSENE-AIR SPRAYS

Spray	$\bar{V}$ cm/sec	u' cm/sec	S_u cm/sec
A	266	22	60
B	↓	↓	72
C	↓	↓	91
D	↓	↓	60
E	↓	↓	50

value of $\bar{d}$ can be calculated and is 54μm. For ϕ = 0.055 and u' = 22 cm/sec, the value of S_u is calculated as 94 cm/sec, and should be compared with the measured value of 60 cm/sec for spray A. The poor agreement is probably due to the poor accuracy of the empirical correlation which was obtained in reference (10) using data with considerable scatter.

CONCLUSIONS

A mathematical model was developed which is capable of predicting the burning velocity in polydisperse air-fuel sprays given the initial conditions of the liquid and gas phases. The analytical predictions were tested against previous experimental data using monodisperse tetralin-air sprays, and the agreement was satisfactory.

The burning velocity in open polydisperse kerosene-air sprays was measured at constant air-fuel ratio and for various degrees of atomization of the spray. The results showed that as the degree of atomization increases, the burning velocity first increases to a maximum value, and then decreases to a burning velocity approaching that of a premixed gas mixture. This result is also predicted by the mathematical model. For one of the sprays tested, it was possible to accurately measure the upstream droplet size distribution. For that spray comparison between measured and calculated burning velocities was satisfactory.

In view of the good agreement between the analytical and experimental predictions, it is concluded that the mathematical model can be used with sprays produced during wind tunnel or field testing of aviation fuels. Calculations using modified fuel sprays produced by wind shear in a wind tunnel will be carried out in the near future when the spray data from the 5 ft wind tunnel at NAFEC becomes available.

Further work is currently being carried out in order to assess experimentally the effect of upstream air and fuel temperature on burning velocity. In addition, a holographic method for particle size measurement is currently being developed. These will provide additional data for checking the theoretical model. Regarding the use of the holographic technique it is expected that it will find useful application during wind tunnel and field spray tests of modified and heat fuels.

APPENDIX A. PROCEDURE FOR CALCULATING THE BURNING VELOCITY IN A LIQUID FUEL SPRAY

A Fortran IV listing of the computer program used for the calculation of burning velocities can be found in Appendix B. Inputs to the program are: (a) Pertinent physical properties for the liquid fuel, fuel vapor, oxygen nitrogen, and the products of combustion which are treated as a single gas, (b) Appropriate values for the activation energy, and pre-exponential rate constant for the fuel vapor reactions, (c) The initial temperature, and droplet size distribution of the spray, (d) The initial air temperature, the velocity difference between the liquid and gas phases, and the intensity and scale of turbulence in the flow, (e) The step size for integration, the velocity step for bracketing a solution, and the position of the high temperature heat source in the grid, (f) Various options for printing intermediate results before the final convergence of the iteration process, and (e) An initial guess for the upstream gas speed. Given the appropriate information, the program goes through an iteration procedure which results in the bracketing of the burning velocity within a predetermined velocity step size.

The listing includes explanatory comments regarding the input quantities, and the following discussion is included as a supplement to these comments.

a) The required physical properties are introduced into the program through a series of READ statements, and also by changing the appropriate statements (as indicated) in subroutine PROPS. The identification of the properties and the appropriate units necessary are included in COMMENT statements.

b) The choice of activation energy, E, and pre-exponential factor, B_o, for the gas phase reactions of kerosene-air mixtures are discussed in a previous section of this report.

c) The initial droplet size distribution can be expressed in terms of a maximum of nine size groups. It is possible to introduce arbitrary drop size distributions or an initial distribution corresponding to the Nukiyama-Tanasawa function.

d) The initial temperature and velocity of the air stream may be different than those of the spray, if desired. It is also necessary for turbulent flows to input the rms velocity fluctuation and Lagrangian turbulence scale of the flow.

e) It is suggested that the position of the high temperature heat source be left in the middle of the integration regime. Convenient step sizes for the velocity step and integration step are 5 cm/sec and 0.003 cm, respectively, the latter depending on the average drop size. Large drops will require a large step size for integration. The number of spacial steps have been set at 200, but this can be changed by changing the DIMENSION statements.

f) The options for printing intermediate results are self explanatory.

g) The upstream gas speed is introduced through the parameter FLOW 1 which is the product of gas speed times the air density. For kerosene-air sprays initially at $300^{o}K$, it is suggested to use FLOW 1 = 0.085 gm/cm^2 sec corresponding to an initial gas speed of about 72 cm/sec.

APPENDIX B. COMPUTER PROGRAM LISTING

```
0001          DIMENSION YF(201),YO(201),YN(201),        YP(201),        DGVG(201
             2),T(201),V(9),CUM(9),VD(9),RE(9),DELT(9),TD(9),EVAP(9),F(9)
             3 ,EMD(201),ENC(201),TDD(9)   ,S(201),RA(201),XF(201,2),XO(201,2),
             4DF(201),DR(201),DD(201),DP(201),DT(201),   DRT(201),E(201),RR(9)
             5,VG(201),FLUX(9),HE(201),G(9),CUI(9),TR(9),VP(9),EVAPR(9),EMR(201)
             6,VDD(9),AR(201),XP(201,2),DFC(201),DFD(201),DFP(201),TTT(201)
             7,VDR(201),TDP(201),ZP(201),ZO(201),ZN(201),Q(201),QQ(9)
0002          COMMON/INIT1/YFI,YOI,YPI,YNI,TI/INIT2/CLDGI//
             2AMF,AMO,AMN,AMP/GEMRL/PR,CON,NJ,VO,DELT,RF,TD,F,
             3FLUX,TB,RR,VDD,TDD/PROF/YF,YO,YN,YP,AM,DGVG,T,VG/SPU/AF,BF
             4/PROP/DIFF,DIFO,DIFP
        C
        C     INPUT PARAMETERS ***********************************************
        C     EXTO=1  USE EXTERNALLY SUPPLIED DROPLET SIZE DISTRIBUTION
        C     EXTO=0.  USE NUKIYAMA-TANASAWA DISTRIBUTION FOR THE DROPLET SISLS
        C     ALPHA  CONSTANT IN NUKIYAMA-TANASAWA DISTRIBUTION
        C     BETA  CONSTANT IN N-T DISTRIBUTION
        C     SAUT  SAUTER MEAN DIAMETER
        C     RANG  RANGE OF VALUES FOR THE RATIO OF DROP DIAMETER TO THE
        C     SAUTER MEAN DIAMETER,MICRONS
        C     DENS  DENSITY OF FUEL IN THE MIXTURE ,GM/CM3
0003          READ 997, EXTO,ALPHA,BETA,SAUT,RANG,DENS
0004     997  FORMAT (6E10.2)
        C     B   PREEXPONENTIAL RATE CONSTANT, SEC-1
        C     AE  ACTIVATION ENERGY,CAL/GM MOLE
        C     Q  HEAT OF REACTION,CAL/GM FUEL
        C     STO  MASS STOICHIOMETRIC COEFFICIENT FOR OXYGEN
        C     HF  STANDARD HEAT OF FORMATION FOR THE GASEOUS FUEL,CAL/GM FUEL
        C     HF  STANDARD HEAT OF FORMATION FOR THE FUEL,CAL/GM FUEL
        C     HP  STANDARD HEAT OF FORMATION FOR THE GASEOUS PRODUCTS,CAL/GM PRO
        C     HFL  STANDARD HEAT OF FORMATION FOR THE LIQUID FUEL,CAL/GM FUEL
        C                  NOTE--HFL=HF-AL
        C     STP  MASS STOICHIOMETRIC COEFFICIENT FOR PRODUCTS
0005          READ 998,B ,AE ,Q,STO,HF,HP,HFL,STP
0006     998  FORMAT(3E10.1,5F10.3)
        C     AF,BF,AO,BO,AN,BN,AP,BP  SPECIFIC HEAT CONSTANTS FOR FUEL
        C     OXIDIZER,NEUTRALS,AND PRODUCTS RESPECTIVELY
        C       NOTE-  CP=A+B*T, CAL/GM-DEG K,  T IN DEG K
0007          READ 999,AF,AO,AP,AN,BF,BO,BP,BN
0008     999  FORMAT(8E10.3)
        C     AMF,AMO,AMN,AMP  MOLECULAR WEIGHTS OF FUEL,OXIDIZER,NEUTRALS,AND
        C     PRODUCTS RESPECTIVELY
        C     PR  GAS PRANDTL NUMBER
        C     TB  LIQUID FUEL BOILING POINT, DEG K
0009          READ 1000,AMF,AMO,AMN,AMP,PR,TB
0010    1000  FORMAT(4F10.2,2F10.5)
        C     RMSU  RMS TURBULENCE FLUCTUATION,CM/SEC
        C     ALG  LAGRANGIAN TURBULENCE SCALE,CM
        C     YFI,YOI,YPI,YNI UPSTREAM SPECIES MASS FRACTIONS
        C     TI  UPSTREAM GAS TEMPERATURE, DEG K
        C     FLOWI  GAS MASS FLUX, GM/CM2-SEC
0011          READ 1001,YFI,YOI,YPI,    YNI,TI,FLOWI,RMSU,ALG
0012    1001  FORMAT(4F10.5,F10.2,3F10.6)
        C      IGAS=1  PRINT ALL GAS PROFILES
        C     IGAS=0   PRINT ONLY FINAL PROFILES
        C     ICO=1  COMPUTE NEXT DROP NUMBER DENSITY
```

```
C       ICO=0  FINISH COMPUTATION AFTER GIVEN NUMBER DENSITY
C       DCO  INCREMENT OF DROPLET NUMBER DENSITY DECREASE
C       DEX INCREMENT OF INTEGRATION, CM
C       N NUMBER OF GRID POINTS
C       L GRID POINT FOR NEAR SOURCE POSITION
0013          READ 1003,DEX,N,L,IGAS,ICO,DCO
0014     1003 FORMAT(F10.5,4I5,I10,F5)
C       DL LIQUID DENSITY, GM/CM3
C       NJ NUMBER OF SIZE GROUPS IN DROPLET SIZE DISTRIBUTION
C       AL LIQUID LATENT HEAT OF VAPORIZATION, CAL/GM
C       CPL LIQUID SPECIFIC HEAT, CAL/GM-DEG K
0015          READ 1004,DL,NJ,AL,CPL
0016     1004 FORMAT(F10.5,I5,2F10.5)
C                THE FOLLOWING CAN BE GIVEN ARBITRARY VALUES IF EXTD=0
C       G(J) DROPLET RADIUS OF GROUP J, CM
C       TR(J) TEMPERATURE OF DROPLET GROUP J, DEG K
C       CO1(J) DROPLET NUMBER DENSITY OF GROUP J,DROPLETS/CM3
C       VR(J) UPSTREAM VELOCITY DIFFERENCE BETWEEN DROPLET OF GROUP J
C       AND THE GAS,  VR(J)=VGAS-VDROPLETS, CM/SEC
0017          READ(5,1005)(G(J),CO1(J),TR(J),VR(J),J=1,NJ)
0018     1005 FORMAT(2E10.5,2F10.5)
C       LFR  POSITION FROM I=1 FOR CHECKING UPSTREAM PROPAGATION
C       IHOLI  INTERVAL FOR PRINTING DROPLET DATA
C       DVEL  VELOCITY CHANGE AFTER A PROFILE CALCULATION  ,CM/SEC
0019          READ 1006,LFR,IHOLI,DVEL,TIGD
0020     1006 FORMAT (2I10,2F10.5)
C       END OF INPUT ***********************************************
0021          TTIG=(0.74*(TD-273)-70.)+273.
0022          IF (EXTD.EQ.1.) GO TO 1116
0023          CALL DISTR (ALPHA,BETA,SAUT,RANG,NJ,G,CO1,DL,DENS)
0024     1116 PCK1=0.
0025          PCK2=0.
0026          PRINT 1007,DL,AL,CPL,AF,BF,AO,DO,AP,BP,AN,BN,B,AE
             1     ,Q,STO,STP,HF,HFL,HP,TB,PP,RMSU,ALG
0027     1007 FORMAT (//T50,'INPUT PARAMETERS'//
             1T5,'DROPLET DENSITY, GM/CM3=',F6.2/T5,'FUEL LATENT HEAT OF VAPORIZ
             2ATION,CAL/GM=', F6.2/T5,'LIQUID FUEL SPECIFIC HEAT, CAL/GM-K=',
             3F6.2/T5,'FUEL VAPOR SPECIFIC HEAT CONSTANTS=',2E15.5/T5,'OXI
             4DIZER SPECIFIC HEAT CONSTANTS=',2E15.5/T5,'PRODUCTS SPECIFIC H
             5EAT CONSTANTS=',2E15.5/T5,'NEUTRALS SPECIFIC HEAT CONSTANTS=',
             62E15.5/T5,'PREEXPONENTIAL CONSTANT,CM3/GM-SEC=',E15.5/T5
             7,'ACTIVATION ENERGY,CAL/GM=',E15.5/T5,'HEAT OF REACTION,CAL/GM=',
             8E15.2/T5,'STOICHIOMETRIC
             9MASS COEFFICIENTS FOR OXIDIZER AND PRODUCTS',2F15.3/T5,
             A'HEAT OF FORMATION FOR THE FUEL VAPOR,CAL/GM=',F15.1/T5,'
             BHEAT OF FORMATION FOR THE LIQUID FUEL,CAL/GM=',F15.1/T5,'
             CHEAT OF FORMATIONFOR THE PRODUCTS,CAL/GM=',F15.1/T5,'LIQUID
             DFUEL BOILING POINT,K=',F15.1/
             ET5,'PRANDTL NUMBER=',F15.3/T5,'RMS TURBULENCE INTENSITY,PERCENT
             F=',F15.3/T5,'LAGRANGIAN SCALE,CM=',F15.3)
0028          GUESS=0.
0029     1106 CALL INTAL (N,DEX       ,PR,L,PCK1,PCK2,     ETA,GUESS)
0030          PRINT 2006
0031          EPSLON=RMSU*ALG*VG(1)
0032     2006 FORMAT(T20,'DROPLET INLET CONDITIONS')
0033          IF (EXTD.EQ.1.) GO TO 2032
```

```
0034          PRINT 2003
0035     2003 FORMAT (T20,'NUKIYAMA-TANASAWA DISTRIBUTION IS USED')
0036          PRINT 2004, ALPHA,BETA
0037     2004 FORMAT (T5,'ALPHA=',F10.2/T5,'BETA=',F10.2)
0038     2002 PRINT 1105
0039     1105 FORMAT(T5,'GROUP',4X,'RADIUS,CM',5X,'NUMBER/CM3',4X,'TEMPERATURE',
            23X,'RELATIVE SPEED,CM/SEC')
0040          PRINT 1008,(J,G(J),CO1(J),TR(J),VR(J),J=1,NJ)
0041     1008 FORMAT(T5,I4,5X,F9.5,3X,F9.0,6X,F5.1,7X,F6.1)
0042          XC1=0.
0043          XC2=0.
0044          DENS1=0.
0045          DO 1107 J=1,NJ
0046          XC1=CO1(J)*((2.*G(J))**3)+XC1
0047     1107 XC2=XC2+CO1(J)*((2.*G(J))**2)
0048          DENS1=DENS1+(XC1*DL*3.14/6.)
0049          DENS=DENS1
0050          IF (XC2.EQ.0.) XC2=1.
0051          DSAUT=XC1/XC2
0052     1108 PRINT 1109,DSAUT,DENS
0053     1109 FORMAT (//T5,'SAUTER MEAN DIAMETER,CM=',E10.2//
            1T5,'FUEL CONCENTRATION,GM/CM3=',E10.2)
C*****************************************************************
C         INITIALIZE VARIABLES
0054          DFL1=DVEL*DGVG(1)
0055          JFINAL=0
0056          KFINAL=0
0057          IFINAL=0
0058          IFL=LFR
0059          TINF=1500.
0060          ISOURC =L
0061          ISOUR1=L+1
0062          LSTOP=0.
0063          IS=1
0064          AMM=1./((YF1/AMF)+(YO1/AMO)+(YP1/AMP)+(YN1/AMN))
0065          DO 1101 I=1,N
0066          ZP(I)=YP(I)
0067          ZO(I)=YO(I)
0068          ZN(I)=YN(I)
0069          ZF(I)=YF(I)
0070          S(I)=0.
0071          EMD(I)=0.
0072          E(I)=0.
0073     1101 ENC(I)=0.
0074     1100 SCK1=0.
0075          SCK2=0.
0076          SCK3=0.
0077          SCK4=0.
0078          COUNT=1
0079          DO 1102 J=1,NJ
0080          QQ(J)=0.
0081          R(J)=G(J)
0082          CON(J)=CO1(J)
0083          TO(J)=TR(J)
0084          TOD(J)=T(J)
0085          RR(J)=G(J)
```

```
0086          1102 VO(J)=(FLOW1/DGVG(I))-VR(J)
0087               ENTHS=0.
0088               FLOWS=0.0
0089               DG=DGVG(I)
0090               VV=VG(I)
0091               C2=YF1*AF+YO1*AO+YN1*AN+YP1*AP
0092               C3=YF1*BF+YO1*BO+YN1*BN+YP1*BP
0093               C4=C2*(T1-298.)+(C3/2)*((T1-298.)**2)
0094               C5=YF1*HF+YP1*HP
0095               H1=C4+C5
0096               HC(I)=H1
0097               C4=C2*(TINF-298.)+(C3/2)*((TINF-298.)**2)
0098               C5=YF1*HF+YP1*HP
0099               HG=C4+C5
0100               I=I
0101               CALL PROPS(YF1,YO1,YP1,YN1,AMM,T1,AK,SHEAT,VISC,EPSLON,DG)
             C*****************************************************************
             C     COMPUTE INLET MASS FLUX AND ENERGY FLUX
0102               DO 1 J=1,NJ
0103               EVAP(J)=0.
0104               DENS=DL*CON(J)*VO(J)*R(J)**3
0105               ENTHJ=CPL*(TO(J)-298.)+HFL
0106               EVAPR(J)=0.
0107               ENTHS=ENTHS+DENS*ENTHJ*(4./3.)*3.14
0108               FLUX(J)=VO(J)*CON(J)
0109          1    FLOWS=FLOWS+DENS*A.*3.14/3.
0110               FLOW=FLOWS+FLOW1
0111               ENA=(HG-H1)*FLOW1
0112               YPINF=((YF1*STP+YP1)*FLOW1+FLOWS*STP)/FLOW
0113               YOINF=((YO1-YF1*STO)*FLOW1-FLOWS*STO)/FLOW
0114               IF (YOINF.LT.0.) YOINF=0.
0115               EM=FLOWS
0116               VG1=(FLOW-FLOWS*(4*3.14/3.))/DGVG(I)
             C*****************************************************************
             C     COMPUTE SPRAY CONDITION AND COUPLING TERMS
0117               IHOLD=IHOLI
0118          2    DG=DGVG(I)
0119               YFF=YF(I)
0120               YOO=YO(I)
0121               YPP=YP(I)
0122               YNN=YN(I)
0123               AMM=1./((YF(I)/AMF)+(YO(I)/AMO)+(YP(I)/AMP)+(YN(I)/AMN))
0124               TT=T(I)
0125               TTT(I)=TT
0126               DO 3 J=1,NJ
0127          3    CON(J)=FLUX(J)/VO(J)
0128               CALL PROPS(YFF,YOO,YPP,YNN,AMM,TT,AK,SHEAT,VISC,EPSLON,DG)
0129               DFP(I)=DIFP
0130               DFO(I)=DIFO
0131               DFF(I)=DIFF
0132               RA(I)=AK/SHEAT
0133               SG=VG(I)
0134               CALL SPORP(DEX,DG,VISC,DL,SG)
0135               CALL RAD(T1, SHEAT,AL,PR,AK,CPL,EVAP,DL,YOO,Q,QO,  STO,EVAPR,1,
                  1AMM,YFF,TIGD)
0136               CALL CPLNG(EVAP,EMOUT,AL,ENCOU,CPL,HFL,SP,SG,EM,DL,EVAPR,CMDOR,
```

```
                 10(X)
0137                SCK1=SCK1+((S(I)-SP)**2)
0138                SCK2=SCK2+((EMD(I)-EMDOUT)**2)
0139                SCK3=SCK3+((HRC(I)-ENCOU)**2)
0140                S(I)=SP
0141                VDR(I)=VD(I)
0142                TDR(I)=TD(I)
0143                EMD(I)=EMDOUT
0144                EMR(I)=EMDOUR
0145                ENC(I)=ENCOU
0146                IF (I.GT.ISOUR1 ) GO TO 4
0147                IF (I.GT.ISOURC ) GO TO 301
0148                SCK4=SCK4+((E(I)-(FLOW-EM))**2)
0149                E(I)=FLOW-EM
0150                GO TO 5
0151          301   SCK4=SCK4+((E(I)-(FLOW-EM))**2)
0152                E(I)=FLOW            -EM
0153                GO TO 5
0154          4     SCK4=SCK4+((E(I)-(FLOW       -EM))**2)
0155                E(I)=FLOW       -EM
0156          5     IF (IS.EQ.1) GO TO 502
0157                GO TO 501
0158          502   IF (I.EQ.1) GO TO 1012
0159          501   IF (I.EQ.IHOLD) GO TO 7
0160          6     GO TO 8
0161          7     II=I
0162                PRINT 1009,II
0163          1009  FORMAT(/T20,'AT SPACE STEP I=',I5)
0164                PRINT 1010
0165          1010  FORMAT(T6,'GROUP',6X,'RADIUS',4X,'NUMBER',3X,'TEMPERATURE',3X,'DRO
                 2P SPEED')
0166                WRITE (6,1011) (J,RR(J),CON(J),TDD(J),VDD(J),J=1,NJ)
0167          1011  FORMAT(T5,I4,5X,F9.5,3X,F5.0,6X,F5.1,7X,F6.1)
0168          1012  PRINT 1013,EMDOUT,EMDOR,ENCOU,SP,EM,E(I)
0169          1013  FORMAT(/T5,'TOTAL EVAPORATION RATE,GM/CM3-SEC=',E15.4/
                 2T5,'REACTIVE EVAPORATION RATE,GM/CM3-SEC=',E15.4/
                 3T5,'SPRAY ENTHALPY FLUX,CAL/CM2-SEC=',E15.4/
                 4T5,'SPRAY VOLUME,CM3LIQUID/CM3 SPACE=',E15.4/
                 5T5,'SPRAY MASS FLUX,GM/CM2-SEC=',E15.4/
                 6T5,'GAS MASS FLUX,GM/CM2-SEC=',E15.4)
0170                IHOLD=IHOLD+2
0171          8     I=I+1
0172                IF(I.GT.N  ) GO TO 1014
0173                GO TO 2
0174          1014  IF (IFINAL.EQ.1) GO TO 204
0175                LT=1
0176                II=1
              C
              C     COMPUTE SPRAY PHASE CONVERGENCE
0177                PRINT 1015,   SCK1,SCK2,SCK3,SCK4
0178          1015  FORMAT (                    T5,'SPRAY VOLUME MEAN SQUARE ERROR=',
                 1E10.3/T5,'EVAPORATION RATE MEAN SQUARE ERROR=',
                 2E10.3/T5,'LIQUID ENTHALPY FLUX MEAN SQUARE ERROR=',E10.3
                 3/T5,'GAS FLUX MEAN SQUARE ERROR=',E10.3///)
0179                SCK=SCK1+SCK2+SCK3+SCK4
0180                IF (SCK.LT.0.1E-2) GO TO 30
```

```
C*****************************************************************
C       COMPUTE GAS PHASE CONDITION
 2000 CONTINUE
      N1=N-1
      DO 11 I=2,N1
      C1=B*(DGVG(I)**2)*EXP(-AE/(1.98*T(I))))*SQRT(T(I))
      TSTOP=T(I)+10.
      IF (T(I).LT.TSTOP) C1=0.
      XF(I,1)=-2.*DEX*E(I)+DGVG(I+1)*DFF(I+1)-DGVG(I-1)*DFF(I-1)
     )-4.*DGVG(I)*DFF(I)
      XO(I,1)=-2.*DEX*E(I)+DGVG(I+1)*DFO(I+1)-DGVG(I-1)*DFO(I-1)
     I-4.*DGVG(I)*DFO(I)
      XP(I,1)=-2.*DEX*E(I)+DGVG(I+1)*DFP(I+1)-DGVG(I-1)*DFP(I-1)
     1-4.*DGVG(I)*DFP(I)
      XF(I,2)=2.*DEX*E(I)-DGVG(I+1)*DFF(I+1)+DGVG(I-1)*DFF(I-1)
     1-4.*DGVG(I)*DFF(I)
      XO(I,2)=2.*DEX*E(I)-DGVG(I+1)*DFO(I+1)+DGVG(I-1)*DFO(I-1)
     1-4.*DGVG(I)*DFO(I)
      XP(I,2)=2.*DEX*E(I)-DGVG(I+1)*DFP(I+1)+DGVG(I-1)*DFP(I-1)
     1-4.*DGVG(I)*DFP(I)
      DF(I)= 8.*DGVG(I)*DFF(I)+4.*DEX*DEX*(EMD(I)+YO(I)*C1)
      DO(I)= 8.*DGVG(I)*DFO(I)+4.*DEX*DEX*(EMD(I)+STO*YF(I)*C1)
   11 DP(I)= 8.*DGVG(I)*DFP(I)+4.*DEX*DEX*EMD(I)
      IF (IT.EQ.1) GO TO 112
C       COMPUTE QUASILINEARIZATION  CONVERGENCE OF THE SPECIES EQUATION
C
      CK3=0.
      DO 165 I=2,N1
      ALHS=YO(I+1)*XO(I,2)+YO(I)*8.*DGVG(I)*DFO(I)+YO(I-1)*XO(I,1)
      ALHS=ALHS/(4.*DEX*DEX)
      C1=B*(DGVG(I)**2)*EXP(-AE/(1.98*T(I))))*SQRT(T(I))
      ARHS=-STO*YF(I)*YO(I)*C1-EMR(I)*STO-EMD(I)*YO(I)
      CK=(ARHS-ALHS)**2
  165 CK3=CK+CK3
      CK3=CK3/(N-2)
      CK1=0.
      DO 110 I=2,N1
      ALHS=YP(I+1)*XP(I,2)+YP(I)*8.*DGVG(I)*DFP(I)+YP(I-1)*XP(I,1)
      ALHS=ALHS/(4.*DEX*DEX)
      C1=B*(DGVG(I)**2)*EXP(-AE/(1.98*T(I))))*SQRT(T(I))
      C1=B*(DGVG(I)**2)*EXP(-AE/(1.98*T(I)))*SQRT(T(I))
      ARHS= STP*YF(I)*YO(I)*C1+EMR(I)*STP-EMD(I)*YP(I)
      CK=(ARHS-ALHS)**2
  110 CK1=CK1+CK
      CK1=CK1/(N-2)
      IF (IT.GT.40 ) GO TO 24
      IF (CK1.LT.1.E-4) GO TO 24
      ROT=0.
  112 IT=IT+1
C       CONTINUE COMPUTATION OF GAS PHASE CONDITION
C       CONSTANTS FOR GAS INTEGRATION
C
 1112 M=N-1
      D1=(-DF(N-1)-XF(N-1,2))/XF(N-1,1)
      DD1=(-DO(N-1)-XO(N-1,2))/XO(N-1,1)
      DDD1=(-DP(N-1)-XP(N-1,2))/XP(N-1,1)
      D2=(-DF(N-2)*D1-XF(N-2,2))/XF(N-2,1)
```

```
0224              DD2=(-DD(N-2)*DD1-XD(N-2,2))/XD(N-2,1)
0225              DDD2=(-DP(N-2)*DDD1-XP(N-2,2))/XP(N-2,1)
0226              N2=N-2
0227              DO 12 I=3,N2
0228              A1=(-DF(N-I)*D2-XF(N-I,2)*D1)/XF(N-I,1)
0229              A2=(-DD(N-I)*DD2-XD(N-I,2)*DD1)/XD(N-I,1)
0230              A3=(-DP(N-I)*DDD2-XP(N-I,2)*DDD1)/XP(N-I,1)
0231              D1=D2
0232              DD1=DD2
0233              DDD1=DDD2
0234              D2=A1
0235              DD2=A2
0236           12 DDD2=A3
         C        PRODUCTS
0237                DO 113 I=2,M
0238              LL=N-I+1
0239          113 DR(LL)=(STP*DX*(DGVG(LL)**2)*YD(LL)*YF(LL)*EXP(-AE/(1.98*
                 1T(LL)))*SQRT(T(LL))+STP*EMR(LL))*4.*DEX*DEX
0240              IP=0.
0241           17 YP(N-1)=YP(N)
0242              DO 18 I=2,M
0243              LL=N-I+1
0244           18 YP(N-I)=(DR(LL)-DP(LL)*YP(LL)-XP(LL,2)*YP(LL+1))/XP(LL,1)
0245              IF (ABS(YP(1)-YP1).LT.0.0005 ) GO TO 133
0246              DELYP=(YP1-YP(1))/A3
0247              YP(N)=YP(N)+DELYP
0248              IP=IP+1
0249              IF (IP.GT.200) GO TO 37
0250              GO TO 17
         C        FUEL SPECIES
0251          133 DO 172 I=2,M
0252              LL=N-I+1
0253              AR(LL)=4.*DEX*DEX*EMR(LL)*(-STO)
0254          172 DR(LL)=4.*(EMD(LL)-EMR(LL))*DEX*DEX
0255           13 YF(N-1)=YF(N)
0256              DO 14 I=2,M
0257              LL=N-I+1
0258              YF(N-I)=(DR(LL)-DF(LL)*YF(LL)-XF(LL,2)*YF(LL+1))/XF(LL,1)
0259           14 CONTINUE
0260              IF(ABS(YF(1)-YF1).LT.0.001  ) GO TO 15
0261              DELYF=(YF1-YF(1))/A1
0262              YF(N)=YF(N)+DELYF
0263              GO TO 13
0264           15 YO(N-1)=YO(N)
0265              DO 16 I=2,M
0266              LL=N-I+1
0267           16 YO(N-I)=(AR(LL)-DD(LL)*YO(LL)-XO(LL,2)*YO(LL+1))/XO(LL,1)
0268              IF(ABS(YO(1)-YO1).LT.0.001  ) GO TO 19
0269              DELYO=(YO1-YO(1))/A2
0270              YO(N)=YO(N)+DELYO
0271              GO TO 15
         C        GAS ENTHALPY
0272           19 CONST2=FLOW1*HE(1)+FLOWS*ENTHS+ENA
0273              T(N)=CONST2/FLOW
0274          102 CONST1=CONS12-ENA
0275              CONST=CONST1
```

```
0276                DO 101 I=1,N
0277            DT(I)=-(E(I)*2.*DEX/(RA(I)))-3.
0278            DTT2=4.
0279            DTT3=-1.
0280            IF (I.GT.1SOURC ) CONST=CONST2
0281        101 DRT(I)=(ENC(I)-ENC(N)-CONST)*2.(DEX/RA(I)
0282            T(N-1)=T(N)
0283            DO 20 I=2,N
0284            LL=N-I
0285         20 T(LL)=(DRT(LL)    -DTT2*T(LL+1)-DTT3*T(LL+2))/DT(LL)
0286            IF (ABS(T(1)-H1).LT.0.05 ) GO TO 22
0287            TT1=1.
0288            TT2=(-DTT2*TT1-DTT3*(2.*DEX*E(N)/(RA(I-2)
               1)))/DT(N-2)
0289            DO 21 I=3,N
0290            A4=(-DTT2*TT2-DTT3*TT1+(2.*DEX*E(N)/(RA(N-I)
               1)))/DT(N-I)
0291            TT1=TT2
0292         21 TT2=A4
0293            DELTT=(T(1)-H1)/A4
0294            T(N)=T(N)+DELTT
0295            CONST2=E(N)*T(N)
0296            GO TO 102
          C     CONVERT  ENTHALPY TO TEMPERATURE
0297         22 DO 103 I=1,N
0298            C3=    (ZF(I)*BF+ZO(I)*BO+ZP(I)*BP+ZN(I)*BN)
0299            C2=ZF(I)*AF+ZO(I)*AO+ZP(I)*AP+ZN(I)*AN
0300            HE(I)=T(I)
0301            IF (C3.EQ.0.) GO TO 104
0302            T(I)=298.+((-C2+SQRT(C2*C2+2.*(T(I)-ZF(I)*HF-ZP(I)*HP)*C3))/C3)
0303            GO TO 103
0304        104 T(I)=298.-((ZF(I)*HF+ZP(I)*HP)/C2)+(T(I)/C2)
0305        103 CONTINUE
0306            TTTI=T(1)+300.
0307            IF (T(IFL).LT.TTTI) GO TO 105
0308            PRINT 1017
0309       1017 FORMAT (///T10,'FLAME PROPAGATES UPSTREAM')
0310            PCKI=1.
0311            GO TO 33
          C     COMPUTE GAS MOLECULAR WEIGHT,DENSITY,SPEED,SP.HEAT
0312        105 DO 23 I=1,N
0313            IF (YP(I).GT.YPINF) YP(I)=YPINF
0314            IF (YP(I).LT.0.) YP(I)=0.
0315            IF (YF(I).LT.0) YF(I)=0.
0316            IF (YO(I).LT.YOINF) YO(I)=YOINF
0317            YN(I)=1.-YF(I)-YO(I)-YP(I)
0318            IF (YN(I).LT.0.) YN(I)=0.
0319            YOO=YO(I)
0320            YPP=YP(I)
0321            YFF=YF(I)
0322            YNN=YN(I)
0323            TT=T(I)
0324            AMM  =1.0/((YFF  /AMF)+(YO(I)/AMO)+(YN(I)/AMN)+(YPP  /AMP))
0325            DGVG(I)=AMM  *(1.0-S(I))/(82.05*T(I))
0326            DG=DGVG(I)
0327            VG(I)=E(I)/DGVG(I)
```

```
      CALL PROPS(YF,YO,YPO,YNN,ARN,TT,AK,SHCAT,VISC,EPSLON,DG)
      DF(I)=DIFF
      DFO(I)=DIFO
      DFP(I)=DIFP
   23 RA(I)=AK/SHCAT
      IF (IGAS.NE.1) GO TO 203
      GO TO 197
  198 IFINAL =1
C     WRITE GAS PROFILES
  197 PRINT 199,IS,IT
  199 FORMAT (1H1,T50,'CYCLE',I5//T50,'GAS PROFILES',I5)
      PRINT 200
  200 FORMAT (T6,'I',8X,'EX',8X,'YF',8X,'YO',8X,'YN',8X,'YP',8X,
     2        'RHO',8X,'T',8X,'VG',8X,'H',6X,'ENDOT',5X,'TOR',4X,'VDR')
      DO 201 I=1,N
      EX= DEX*(I-L)
      YPP=YP(I)
      YFF=YF(I)
  201 PRINT 202,I,EX,YFF,  YO(I),YN(I),       YPP,          DGVG(I),T(I),
     2VG(I),HE(I),EMD(I),TDR(I),VDR(I)
  202 FORMAT (T3,I4,F11.3,4F10.4,       F10.4,3F10.2,F10.6,F8.2,F6.1)
      IF (JFINAL.EQ.1) GO TO 333
      IF (IFINAL.EQ.1) GO TO 1100
  203 GO TO 2000
   24 CONTINUE
C     COMPUTE CONVERGENCE OF ENERGY EQUATION
      CK2=0.
      CONST=CONST1
      DO 25 I=1,N2
      IF (I.GT.L) CONST=CONST2
      ARHS=(ENC(I)-ENC(N)-CONST)
      ALHS=E(I)*HE(I)-RA(I)          *((-3*HE(I)+4.*HE(I+1)-HE(I+2))/
     1(2.*DEX))
      ALHS=-ALHS
      CK=(ALHS-ARHS)**2
   25 CK2=CK2+CK
      CK2=CK2/(N-2)
      IF (LT.GT.20 ) GO TO 27
      IF (CK2.LT.1.E-2) GO TO 27
      LT=LT+1
      GO TO 1112
   27 CK=0.
      DO 28 I=1,N
   28 CK=CK+(YP(I)-ZP(I))**2
      DO 298 I=1,N
      ZP(I)=YP(I)
      ZO(I)=YO(I)
      ZN(I)=YN(I)
  298 ZF(I)=YF(I)
      IF (CK.LT.5.E-3) GO TO 299
      IT=1
      LT=1
      GO TO 2000
  299 PRINT 29,IT,CK3,CK2,CK
   29 FORMAT (T5,'QUAZILINEZRIZATION CONVERGENCE AT ITERATION NUMBER=',
     1I5/T5,'OXIDIZER EQUATION MEAN SQUARE ERROR=',E10.3/T5,'ENERGY EQUA
```

```
     21ION MEAN SQUARE ERROR=',E10.3/T5,'PRODUCTS EQUATION MEAN SQUARE E
     3ROR=',E10.3)
      IS=IS+1
      GO TO 1100
   30 PRINT 31
   31 FORMAT (///T5,'LAST CYCLE SATISFIES LIQUID PHASE EQUATIONS')
      IF (IGAS.EQ.0) GO TO 198
  204 RYP1=YP(N)*R(N)
      RYP2=FLOW2*STP+(YF)*STP+YP1)*FLOW1
      RATIOP=RYP1/RYP2
      PRINT 331,RATIOP
  331 FORMAT (/T5,'RATIO OF PRODUCTS OUT OVER PRODUCTS COMPUTED BY
     1STOICHIOMETRY',F10.5)
      PCK2=2.
      IF (PCK1.EQ.1) GO TO 35
      FLOW2=FLOW2-FLOW2*(DFL1/FLOW1)
      FLOW1=FLOW1-DFL1
      DO 32 J=1,NJ
      VD(J)=(FLOW1/DGVG(1))-VR(J)
      GUESS=1.
   32 IF (VD(J).LT.0.) KFINAL=1
      IF (KFINAL.EQ.1) GO TO 37
      VG(1)=FLOW1/DGVG(1)
      GO TO 1106
   33 IF (PCK2.EQ.2) GO TO 35
      JFINAL=1
      GO TO 197
  333 FLOW2=FLOW2+FLOW2*(DFL1/FLOW1)
      FLOW1=FLOW1+DFL1
      DO 34 J=1,NJ
   34 VD(J)=(FLOW1/DGVG(1))-VR(J)
      GUESS=0.
      JFINAL=0
      GO TO 1106
   35 PRINT 36
   36 FORMAT (//5X,'FLAME PROPAGATION VELOCITY LIES BETWEEN THE LAST
     1TWO VALUES OF FLOW1 ATTEMPTED')
      IF (ICO.EQ.0) GO TO 37
      CO1(1)=CO1(1)-OCO
       IF (CO1(1).EQ.0.) GO TO 37
      GO TO 1116
   37 STOP
      END
```

```
0001          SUBROUTINE INTAL (N,DEX        ,PR,L,PCK1,PCK2,     ENA,GUESS)
0002          DIMENSION YF(201),YO(201),YN(201),          YP(201),          DA(201),
             2T(201),VG(201)
0003          COMMON/INIT1/YF1,YO1,YP1,YN1,T1/INIT2/FLOW1//
             2AMF,AMO,AMN,AMP/PROF/YF,YO,YN,YP,AM,DA,T,VG
0004          FLOW=FLOW1
0005          TINF=1500.
0006          ENA=TINF*FLOW*0.24
0007          IF (GUESS.EQ.1.) GO TO 9
0008          C6=TINF-T1
0009          LN=L+1D
0010          DO 1 I=1,L
0011          YF(I)=YF1
0012          YO(I)=YO1
0013          YN(I)=YN1
0014          YP(I)=YP1
0015          EX=FLOAT(I-LN)/FLOAT(L-LN)
0016          IF (I.GT.LN) GO TO 20
0017          T(I)=T1
0018          GO TO 21
0019       20 YF(I)=YF1
0020          YO(I)=YO1
0021          YN(I)=YN1
0022          YP(I)=YP1
0023          T(I)=T1+C6*EX
0024       21 AMN  =1.0/((YF(I)/AMF)+(YO(I)/AMO)+(YN(I)/AMN)+(YP(I)/AMP))
0025          DA(I)=AMN  /(82.05*T(I))
0026       1  VG(I)=FLOW1/DA(I)
0027          AMINF=AMN
0028          DAINF=AMINF/(82.05*TINF)
0029          NNN=N-L
0030          DO 2 I=1,NNN
0031          J=I+L
0032          YF(J)=YF1
0033          YO(J)=YO1
0034          YN(J)=YN1
0035          YP(J)=YP1
0036          T(J)=TINF
0037          DA(J)=DAINF
0038       2  VG(J)= FLOW1/DA(J)
0039       9  PRINT 10
0040       10 FORMAT('1',T20,'UPSTREAM CONDITIONS')
0041          PRINT 11,FLOW1,YF1,YO1,YP1,YN1,T1
0042       11 FORMAT(T2,'UPSTREAM'/T12,'GAS MASS FLOW RATE=',F7.5/T12,'FUEL MASS
             2FRACTION=',F6.3/T12,'OXIDIZER MASS FRACTION=',F6.3/T12,'PRODUCTS M
             3ASS FRACTION=',F6.3/T12,'NEUTRALS MASS FRACTION=',F6.3
             4                                  /T12,'TEMPERATURE=',F7.2)
0043          PRINT 13,AMF,AMO,AMN,AMP
0044       13 FORMAT(T20,'MOLECULAR WEIGHTS'/T12,'FUEL=',F6.2/T12,'OXIDIZER=',F5
             2.2/T12,'NEUTRAL=',F5.2/T12,'PRODUCTS=',F6.2)
0045          PRINT 14,DEX
0046       14 FORMAT(T20,'STEP SIZES'/T12,'SPACE STEP FOR GAS INTEGRATION=',F8.5
             2//)
0047          PRINT 15
0048       15 FORMAT(T50,'INITIAL PROFILE GUESS')
0049          PRINT 16
```

```
   16 FORMAT(T16,'I',8X,'EX',8X,'YF',8X,'YO',8X,'YN',8X,'YP',8X,
     2        'RHO',8X,'T',8X,'VG')
      DO 3 I=1,N
      EX= DEX*(I-L)
    3 PRINT 17,I,EX,YF(I),YO(I),YN(I),       YP(I),       DA(I),T(I),VG(I)
   17 FORMAT(T13,I4,F11.3,4F10.4,       F10.4,2F10.2)
   18 CONTINUE
      RETURN
      END
```

```
0001          SUBROUTINE PROPS (YF,YO,YP,YN,AMM,T,CMIX,CPMIX,VISC,EPSLON,DG)
        C     THIS SUBROUTINE COMPUTES THE MIXTURE SPECIFIC HEAT, THERMAL CON-
        C     DUCTIVITY, VISCOSITY, AND DIFFUSION COEFFICIENTS OF EACH SPECIES
0002          DIMENSION C1(3),C2(3), C3(3),C4(3),C5(3),C6(3),TB(3),AM(3)
             1 ,CP(3),AK(3),V(3),Y(3)
0003          COMMON/PROP/DIFF,DIFO,DIFP//AMF,AMO,AMN,AMP
        C     C3(1), C4(1) SPECIFIC HEAT CONSTANTS FOR THE FUEL VAPOR
        C     C3(2),C4(2)  SPECIFIC HEAT CONSTANTS FOR THE OXIDIZER
        C     C3(3),C4(3)  SPECIFIC HEAT CONSTANTS FOR THE PRODUCTS
        C         NOTE- C3(I)+C4(I)*T=CP,T IN DEG R, CP IN CAL/GM-DEG K
        C     C1(1),C2(1) THERMAL CONDUCTIVITY CONSTANTS FOR THE FUEL VAPOR
        C     C1(2),C2(2) THERMAL CONDUCTIVITY CONSTANTS FOR OXYGEN
        C     C1(3),C2(3) THERMAL CONDUCTIVITY CONSTANTS FOR NEUTRAL S
        C        NOTE - C1(I)+C2(I)=K, T IN DEG R, K IN BTU/HR-FT-DEG R
        C     C5(1),C6(1) VISCOSITY CONSTANTS FOR THE FUEL VAPOR
        C     C5(2),C6(2) VISCOSITY CONSTANTS FOR THE OXIDIER
        C     C5(3),C6(3) VISCOSITY CONSTANTS FOR THE PRODUCTS
        C         NOTE- C5(I)+C6(I)=V, T IN DEG R, V IN LB/FT-SEC
0004          T1=T*9./5.
0005          C1(1)=-6.6E-3
0006          C1(2)=11.E-3
0007          C2(1)=26.3E-6
0008          C2(2)=17.78E-6
0009          C1(3)=7.7E-3
0010          C2(3)=17.73E-6
0011          C3(1)=0.097
0012          C4(1)=0.55E-3
0013          IF (T1.LT.1000.) GO TO 3
0014          IF (T1.GT.1700.) GO TO 4
0015          C3(1)=0.314
0016          C4(1)=0.336E-3
0017          GO TO 3
0018        4 C3(1)=0.585
0019          C4(1)=0.175E-3
0020        3 C3(2)=224.E-3
0021          C4(2)=19.3E-6
0022          C3(3)=281.6E-3
0023          C4(3)=6.7E-6
0024          C5(1)=105.E-7
0025          C6(1)=75.E-10
0026          C5(2)=136.E-7
0027          C6(2)=101.91E-10
0028          C5(3)=131E-7
0029          C6(3)=95.19E-10
0030          AM(1)=AMF
0031          AM(2)=AMO
0032          AM(3)=AMN
0033          Y(1)=YF
0034          Y(2)=YO
0035          Y(3)=YP+YN
        C     CONVERT PROPERTIES TO THE CORRECT UNITS
0036          DO 1 I=1,3
0037          AK(I)=(C1(I)+C2(I)*T1)*0.0041336
0038          CP(I)=C3(I)+C4(I)*T1
0039        1 V(I)=(C5(I)+C6(I)*T1)*14.881
0040          CPMIX=0.
```

```
      CMIX=0.
      VISC=0.
      DO 2 I=1,3
      CPMIX=CPMIX+CP(I)*Y(I)
      XI=Y(I)*AMM/AM(I)
      CMIX=CMIX+AK(I)*XI
    2 VISC=VISC+V(I)*XI
      CMIX=CMIX+LPSL(N)*CPMIX*DG
C     CALCULATION OF THE SPECIES DIFFUSION COEFFICIENTS USING THE SLATTERY
C     FORMULA.  BINARY DIFFUSION COEFFICIENTS ARE FOR EACH OF THE SPECIES IN A
C     TCO CRITICAL TEMPERATURE FOR OXYGEN,DEG K
C     TCF CRITICAL TEMPERATURE FOR FUEL ,DEG K
C     PCO CRITICAL PRESSURE FOR OXYGEN,ATM
C     PCP CRITICAL PRESSURE FOR THE PRODUCTS,ATM
C     PCA CRITICAL PRESSURE FOR AIR,ATM
C     PCF CRITICAL PRESSURE FOR FUEL,ATM
      TCP=304.
      TCA=132.
      TCO=154.
      TCF=740.
      PCA=37.
      PCP=73.
      PCO=50.
      PCF=40.
      CONST=(2.74E-4)*(T**1.823)
      DIFF=CONST*SQRT((AMF+AMM)/(AMF*AMM))*((PCF*PCA)**0.333)/
     1 ((TCF*TCA)**0.495)
      DIFO=CONST*SQRT((AMO+AMM)/(AMO*AMM))*((PCO*PCA)**0.333)/
     1 ((TCO*TCA)**0.495)
      DIFP=CONST*SQRT((AMP+AMM)/(AMP*AMM))*((PCP*PCA)**0.333)/
     1 ((TCP*TCA)**0.495)
      DIFF=DIFF+LPSLON
      DIFO=DIFO+LPSLON
      DIFP=DIFP+LPSLON
      RETURN
      END
```

```
0001          SUBROUTINE RAD(TT, SHEAT,AL,PR,AK,CPL,EVAP,DL,DX,Q,QQ,  STO,EVAPP,
             1I,AMM,YFF,TIGO)
        C     THIS SUBROUTINE COMPUTES THE TEMPERATURE, RADIUS CHANGE, AND
        C     EVAPORATION RATE FOR EACH DROPLET SIZE GROUP.
0002          DIMENSION R(9),CON(9),DELT(9),RE(9),TD(9),EVAP(9),VD(9),F(9),
             1FLUX(9),EVAPR(9),TIG(9),RP(9),VDD(9),TDD(9),QQ(9)
0003          COMMON /GENRL/R,CON,NJ,VD,DELT,RE,TD,F,FLUX,TB,PR,VDD,TDD/SPD/AF,
             1BF//AMF,AMD,AMN,AMP
0004          AR=AL/1.98
0005          AM=AMM
0006          YF=YFF
0007          TC=TB-5.
0008          DO 2 J=1,NJ
0009          RATIO=1.+0.3*(PR**0.33)*SQRT(RE(J))
0010          EVAPR(J)=0.
0011          TIG(J)=(0.74*(TB-273.)-70.)+273.
0012          T=TD(J)
0013          TDD(J)=T
0014          IF (TT.LT.TIGO) GO TO 9
0015          IF (TD(J).GT.TIG(J)) QQ(J)=0
0016          IF (QQ(J).LT.0) GO TO 9
0017     20   DRDT=ALOG(1.+(SHEAT*(TT-TD(J))/AL)+(QQ(J)*DX/(STO*AL)))
0018          GO TO 11
0019      9   IF (TD(J).LT.TC) GO TO 19
0020          GO TO 20
0021     19   EX=EXP(AMF*AR*(TD(J)-TB)/(TD(J)*TB))
0022          YFS=AMF*EX/(AN-(AM-AMF)*EX)
0023          DRDT=(YFS-YF)/(1.-YFS)
0024          IF (DRDT.LT.0. ) DRDT=0.
0025          CPFS=AF+BF*TD(J)
0026          ZETA=ALOG(1.+(CPFS/SHEAT)*DRDT)
0027          IF (ZETA.LT.1.) GO TO 11
0028          DRDT=DRDT*(ZETA/(EXP(ZETA)-1.))
0029     11   H=RATIO*AK/R(J)
0030          EVAP(J)=RATIO*DRDT*4.*3.14*R(J)*AK/SHEAT
0031          IF (EVAP(J).EQ.0.) GO TO 31
0032          CPFS=AF+BF*TD(J)
0033          ZETA=EVAP(J)*CPFS/(0.28*R(J)*2.*RATIO)
0034          IF (ZETA.LT.0.1) GO TO 31
0035          CZET=ZETA/(EXP(ZETA)-1.)
0036          H=H*CZET
0037     31   F1=          ((3.*H*(TT-TD(J))/(CPL*DL*R(J)))-     (
             1EVAP(J)*AL*3./(4.*3.14*(R(J)**3)*CPL*DL)))*DELT(J)
0038          H=RATIO*AK/R(J)
0039          TD(J)=TD(J)+F1
0040          IF (TD(J).GT.TB) TD(J)=TB
0041          IF (TT.LT.TIGO) GO TO 15
0042          IF (QQ(J).LT.0) GO TO 15
0043     22   DRDT=ALOG(1.+(SHEAT*(TT-TD(J))/AL)+(QQ(J)*DX/(STO*AL)))
0044          GO TO 6
0045     15   IF (TD(J).LT.TC) GO TO 21
0046          GO TO 22
0047     21   EX=EXP(AMF*AR*(TD(J)-TB)/(TD(J)*TB))
0048          YFS=AMF*EX/(AM-(AM-AMF)*EX)
0049          DRDT=(YFS-YF)/(1.-YFS)
0050          IF (DRDT.LT.0. ) DRDT=0.
```

```
      CPFS=AF+BF*TD(J)
      ZETA=ALOG(1.+(CPFS/SHEAT)*DRDT)
      IF (ZETA.LT.0.1) GO TO 6
      DRDT=DRDT*(ZETA/(EXP(ZETA)-1.))
    6 EVAP(J)=RATIO*DRDT*4.*3.14*R(J)*AK/SHEAT
      IF (EVAP(J).EQ.0.) GO TO 61
      CPFS=AF+BF*TD(J)
      ZETA=EVAP(J)*CPFS/(6.28*R(J)*2.*RATIO)
      IF (ZETA.LT.0.1) GO TO 61
      CZET=ZETA/(EXP(ZETA)-1.)
      H=H*CZET
   61 F2=          ((3.414*(TT-TD(J))/(CPL*DL*R(J)))-     (
     1EVAP(J)*AL*J./(4.*3.14*(R(J)**3)*CPL*DL)))*DELT(J)
      TD(J)=T+(F2/2)*0.5
      IF (TD(J).GT.TB) TD(J)=TB
      IF (TT.LT.T100) GO TO 17
      IF (QQ(J).LT.0) GO TO 17
   24 DRDT=ALOG(1.+(SHEAT*(TT-TD(J))/AL)+(QQ(J)*QX/(STG*AL)))
      GO TO 8
   17 IF (TD(J).LT.TC) GO TO 23
      GO TO 24
   23 EX=EXP(AMF*AR*(TD(J)-TB)/(TD(J)*TB))
      YFS=AMF*EX/(AM-(AM-AMF)*EX)
      DRDT=(YFS-YF)/(1.-YFS)
      IF (DRDT.LT.0. ) DRDT=0.
      CPFS=AF+BF*TD(J)
      ZETA=ALOG(1.+(CPFS/SHEAT)*DRDT)
      IF (ZETA.LT.0.1) GO TO 8
      DRDT=DRDT*(ZETA/(EXP(ZETA)-1.))
    8 EVAP(J)=RATIO*DRDT*4.*3.14*R(J)*AK/SHEAT
      R1=R(J)
      DRDT=EVAP(J)/(4.*3.14*DL*R(J)*R(J))
      DR1=DRDT
      R(J)=R(J)-DRDT*DELT(J)
      IF(R(J).LT.0.0) GO TO 10
      DRDT=EVAP(J)/(4.*3.14*DL*R(J)*R(J))
      R(J)=R1-(DRDT+DR1)*0.5*DELT(J)
   10 IF (R(J).LT.0.) GO TO 13
      GO TO 14
   13 R(J)=0.
   14 IF (I.EQ.1) RR(J)=R(J)
      EVAP(J)=4.*3.14*(R1**2)*(RR(J)-R(J))*DL/(DELT(J)*2)
      RR(J)=R1
      IF (TT.LT.T100) GO TO 12
      IF (QQ(J).LT.0) GO TO 12
      LVAPR(J)=EVAP(J)
   12 IF (R(J).EQ.0.) GO TO 1
      GO TO 2
    1 R(J)=1.0
      TD(J)=TC
      FLUX(J)=0.
    2 CONTINUE
      RETURN
      END
```

```
0001          SUBROUTINE SPDRP(DEX,DG,VISC,DL,VG)
        C     THIS SUBROUTINE COMPUTES THE DROP SPEED,VD,AT EX*DEX, THE TIME FOR
        C     EACH SPACE STEP,DELT, AND THE REYNOLDS NUMBER,RE.
0002          DIMENSION R(9),CON(9),VD(9),RE(9),DELT(9),TD(9),F(9),FLUX(9)
             1,RR(9),VDD(9),TDD(9)
0003          COMMON/GENRL/R,CON,NJ,VD,DELT,RE,TD,F,FLUX,TB,RR,VDD,TDD
        C
        C     DELT(J)=TIME STEP FOR EACH DROPLET GROUP
        C     RE(J)=REYNOLDS NUMBER FOR EACH DROPLET GROUP
        C     VD(J)=SPEED OF EACH DROPLET GROUP
        C     VG=GAS VELOCITY
0004          DO 2 J=1,NJ
0005          V=VD(J)
0006          VDD(J)=V
0007          DELT(J)=DEX/VD(J)
0008          C2=ABS(VG-VD(J))
0009          RE(J)=2.*R(J)*C2*DG/VISC
0010          IF (RE(J).EQ.0.) GO TO 1
0011          CD=27./(RE(J)**0.84)
0012          F(J)=(3./8.)*CD*DG*C2*(VG-VD(J))/(R(J)*DL)
0013          GO TO 3
0014      1   F(J)=0.
0015      3   F1=F(J)
0016          VD(J)=VD(J)+DELT(J)*F(J)
0017          C2=ABS(VG-VD(J))
0018          RE(J)=2.*R(J)*C2*DG/VISC
0019           IF (RE(J).EQ.0.) GO TO 4
0020          CD=27./(RE(J)**0.84)
0021          F(J)=(3./8.)*CD*DG*C2*(VG-VD(J))/(R(J)*DL)
0022          GO TO 2
0023      4   F(J)=0.
0024          VD(J)=V+0.5*(F(J)+F1)*DELT(J)
0025      2   RE(J)=2.*R(J)*ABS(VG-V)*DG/VISC
0026          RETURN
0027          END
```

```
0001          SUBROUTINE DISTR(ALPHA,BETA,SAUT,RANG,J,R,CONC,DL,DENS)
        C     THIS SUBROUTINE CALCULATES THE DROP SIZES USING THE NISHIWAKI-
        C     TANASAWA DISTRIBUTION FUNCTION
0002          DIMENSION R(9),CONC(9)
0003          C1=ALPHA+4
0004          C2=ALPHA+3
0005          C3=GAMMA(C1/BETA)
0006          C4=GAMMA(C2/BETA)
0007          A=BETA*(C3**C2)/(C4**C1)
0008          B=(C3/C4)**BETA
0009          DENS1=0.
0010              DO 1  I=1,J
0011          D=(SAUT+RANG/J )*I
0012          RATIO=D/SAUT
0013          F=A*(RATIO**C2)*EXP(-B*(RATIO**BETA))
0014          R(I)=D/2.
0015          DENN    =DENS*F*RANG/J
0016          CONC(I)=3*DENN/(4.*3.14*(R(I)**3)*DL)
0017          II=IFIX(CONC(I))
0018          CONC(I)=II
0019        1 DENS1=DENS1+(4.*3.14*(R(I)**3)*DL*CONC(I)/3.)
0020          CK=ABS(DENS-DENS1)
0021          IF (CK.LT.1.E-6) GO TO 3
0022          DO 2 I=1,J
0023        2 CONC(I)=CONC(I)*((DENS-DENS1)/DENS)
0024          II=IFIX(CONC(I))
0025          CONC(I)=II
0026        3 RETURN
0027          END
```

```
0001          SUBROUTINE CPL(EVAP,EMDOT,AL,ENCOU,CPL,HFL,SP,VG,L,DL,EVAPR,
             1EMDOR,DEX)
        C
        C     THIS SUBROUTINE COMPUTES THE COUPLING TERMS FOR EACH SPACE STEP
        C     EMDOT= TOTAL EVAPORATION RATE,G/CM3-SEC
        C     ENCOU= TOTAL ENERGY ADDITION DUE TO EVAPORATING MASS OF FUEL,CAL/C
        C     SP= SPRAY VOLUME,CM3 LIQUID/CM3 SPACE
        C
0002          DIMENSION R(9),CON(9),DELT(9),RP(9),TD(9),EVAP(9),VD(9),F(9)
             1,FLUX(9),EVAPR(9),PC(9),VDD(9),TDD(9)
0003          COMMON/GENRL/R,CON,NJ,VD,DELT,RE,TD,F,FLUX,TB,RR,VDD,TDD
0004          ENCOU=0.
0005          EMDOT=0.
0006          EMDOR=0.
0007          SP=0.
0008          DO 1 J=1,NJ
0009          C1=EVAP(J)*CON(J)
0010          CC1=(VAPR(J)*CON(J)
0011          EMDOT=EMDOT+C1
0012          EMDOR=EMDOR+CC1
0013          ENTH=CPL*(TDD(J)-298.)+HFL
0014          C2=(RP(J)**3)*CON(J)*(4.*3.14/3.)
0015          ENCOU=ENCOU+ENTH*C2*DL*VDD(J)
0016        1 SP=SP+C2
0017          E=E-EMDOT*DEX
0018          RETURN
0019          END
```

REFERENCES

1. Burgoyne, J. H., and Cohen, L., "The Effect of Drop Size on Flame Propagation in Liquid Aerosols," Proc. Roy. Soc. of London, A, 225, p. 375 (1954).

2. Burgoyne, J. H., "Mist and Spray Explosions," Ch. Eng. Prog., 53, p. 121 (1957).

3. Mizutani, Y., and Ogasawara, M., "Laminar Flame Propagation in Droplet Suspension of Liquid Fuel," Int. J. Ht. M. Tr., 6, p. 921 (1965).

4. Polymeropoulos, C. E., "Flame Propagation in a One-Dimensional Liquid Fuel Spray," Comb. Sci. Tech., 9, p. 5,6 (1974).

5. Polymeropoulos, C. E., Das, S., and Merrill, B., "Observations on the Burning Velocity of Kerosene-Air sprays," Eastern Section of the Combustion Institute, John Hopkins, Nov. 1974.

6. Williams, F. A., "Monodisperse Spray Deflagration," Progress in Astronautics and Rocketry, 2, p. 223 (1966).

7. Wood, B. J., Rosser, W. A., and Wise, H., "The Ignition and Combustion of Drops in Sprays of No. 2 Heating Oil," API Conference on Distillate Fuel Combustion, Chicago, (1963).

8. Cekalin, E. K., "Propagation of Flame in Turbulent Flow of Two Phase Fuel-Air Mixture," Eighth Symp. on Comb., Williams and Wilkins, New York, 1962, p. 1125.

9. Mizutani, Y., and Nishimoto, T., "Turbulent Flame Velocities in Premixed Sprays. Part I - Experimental Study," Comb. Sci. Tech., 6, p. 1 (1972).

10. Mizutani, Y., and Nakajima, A., "Combustion of Fuel Vapor-Drop-Air Systems. Part I - Open Burner Flames," Comb. and Flame, 10, p. 343 (1973).

11. Dickinson, D. R., and Marshall, W. R., "The Rates of Evaporation of Sprays," AIChE J., 14, p. 541 (1968).

12. Nuruzzaman, A. S. M., Siddall, R. G., and Beer, J. M., "The Use of Simplified Mathematical Model for Prediction of Burnout of Non-Uniform Sprays," Ch. Engr. Sci., 26, p. 1635, (1971).

13. Mizutani, Y., "Turbulent Flame Velocities in Premixed Sprays. Part II - Theoretical Analysis," Comb. Sci. Tech., 6, p. 11 (1972).

14. Sutton, R. D., Hines, W. S., and Combs, L. P., "Comprehensive Analysis of Liquid Rocket Combustion," AIAA paper No. 70-622, San Diego, June 1970.

15. Suppramaniam, S., "Ignition Delay of Individual Liquid Fuel Droplets," Ind. Eng. Chem., Proc. Des. and Development, 10, p. 297 (1971).

16. Priem, R. J., Borman, G. L., El-Wakil, M. M., Uyehara, D. A., and Myers, P. S., "Experimental and Calculated Histories of Vaporizing Drops," NACA TN-3988, (1957).

17. Ranz, W. E., and Marshall, W. R., "Evaporation from Drops," Chem. Engr. Prog., 48, p. 141 (1952).

18. Rosner, D. E., "Liquid Droplet Vaporization and Combustion," Liquid Propellant Rocket Combustion Instability, NASA SP-194, p. 198 (1972).

19. Law, C. K., and Williams, F. A., "Kinetics and Convection in the Combustion of Alkane Droplets," Comb. and Flame, 19, p. 393 (1972).

20. Faeth, G. M., and Lazar, R. S., "Bibropellant Droplet Burning Rates and Lifetimes in a Combustion Environment," NASA CR-72622 (1969).

21. Fay, J. A., and Kaye, H., "A Finite Difference Solution of Similar Non-Equilibrium Boundary Layers," AIAA J., 5, p. 1949 (1967).

22. "Handbook of Chemistry and Physics," The Chemical Rubber Co., Cleveland, 1967.

23. Fristrom, R. M., and Westenberg, A. A., "Flame Structure," McGraw-Hill, New York, 1965, p.23.

24. Anson, D., "Influence of the Quality of Atomization on the Stability of Combustion of Liquid Fuel Sprays," Fuel, 32, p. 39 (1953).

25. Whittle, J., "Effect of Vaporization Rate on the Weak Combustion Limit of Liquid Fuel Sprays," Fuel, 33, p. 193 (1954).

26. Ingebo, R. D., "Vaporization Rates and Drag Coefficients for Iso-octane Sprays in Turbulent Air Streams," NACA TN-3265, (1954).